Coupled states of electromagnetic fields with magnetic-dipolar-mode vortices: Magnetic-dipolar-mode vortex polaritons

E. O. Kamenetskii, R. Joffe, and R. Shavit
Department of Electrical and Computer Engineering, Ben Gurion University of the Negev, Beer Sheva, Israel
(Received 9 December 2010; published 19 August 2011)

A coupled state of an electromagnetic field with an electric or magnetic dipole-carrying excitation is well known as a polariton. Such a state is the result of the mixing of a photon with the excitation of a material. The most discussed types of polaritons are phonon polaritons, exciton polaritons, and surface-plasmon polaritons. Recently, it was shown that, in microwaves, strong magnon-photon coupling can be achieved due to magnetic-dipolar-mode (MDM) vortices in small thin-film ferrite disks. These coupled states can be specified as MDM-vortex polaritons. In this paper, we study the properties of MDM-vortex polaritons. We numerically analyze a variety of topological structures of MDM-vortex polaritons. Based on analytical studies of the MDM spectra, we give theoretical insight into a possible origin for the observed topological properties of the fields. We show that the MDM-vortex polaritons are characterized by helical-mode resonances. We demonstrate the $\mathcal{PT}$-invariance properties of MDM oscillations in a quasi-two-dimensional ferrite disk and show that such properties play an essential role in the physics of the observed topologically distinctive states with the localization or cloaking of electromagnetic fields. We may suppose that one of the useful implementations of the MDM-vortex polaritons could be microwave metamaterial structures and microwave near-field sensors.

DOI: 10.1103/PhysRevA.84.023836 PACS number(s): 42.25.Fx, 42.25.Bs, 76.50.+g

I. INTRODUCTION

The coupling between photons and magnons in a ferromagnet has been studied in many works over a long period of time. In an assumption that there exists an oscillating photon field associated with the spin fluctuations in a ferromagnet, one can observe the photonlike and magnonlike parts in the dispersion relations. The dispersion characteristics for the coupled magnon-photon modes were analyzed for various directions of the incident electromagnetic wave vector, and it was found, in particular, that there are reflectivity bands for electromagnetic radiation incident on the ferromagnet-air interface [1–4]. As one of the most attractive effects in studies of the reflection of electromagnetic waves from magnetic materials, there is the observation of a nonreciprocal phase behavior [5].

In the general case of oblique incidence on a single ferrite-dielectric interface, apparently different situations arise by changing the directions of incident waves and bias and the incident side of the interface. The solutions obtained for different electromagnetic problems of ferrite-dielectric structures show the time-reversal symmetry-breaking (TRSB) effect [6–10]. Microwave resonators with the TRSB effect give an example of a nonintegrable electromagnetic system. In general, the concept of nonintegrable, i.e., path-dependent phase factors is considered as one of the fundamental aspects of electromagnetism. The path-dependent phase factors are the reason for the appearance of complex electromagnetic-field eigenfunctions in resonant structures with enclosed ferrite samples, even in the absence of dissipative losses. In such structures, the fields of eigenoscillations are not the fields of standing waves despite the fact that the eigenfrequencies of a cavity with a ferrite sample are real [11]. Because of the TRSB effect and the complex-wave behaviors, one can observe induced electromagnetic vortices in microwave resonators with ferrite inclusions [12–14].

Very interesting effects appear when an oscillating photon field is coupled with the resonant collective-mode behavior of spin fluctuations in a confined ferromagnetic structure. This concerns, in particular, a microwave effect of strong coupling between electromagnetic fields and long-range magnetic dipolar oscillations. Such oscillations, known as magnetic-dipolar-mode (MDM) or magnetostatic (MS) oscillations, take place due to the long-range phase coherence of precessing magnetic dipoles in ferrite samples. The wavelength of MDM oscillations is 2–4 orders of magnitude less than the free-space electromagnetic wavelength at the same microwave frequency [11]. The fields associated with MDM oscillations in confined magnetic structures decay exponentially in strength with increasing distance from the ferrite-vacuum interface. In general, these modes are nonradiative. The nonradiative character of MDMs has two important consequences: (i) MDMs cannot couple directly to photonlike modes (in comparison to photonlike modes, the MDM wave vectors are too great), and (ii) the fields associated with MDMs may be considerably enhanced in strength in comparison to those used to generate them. The electromagnetic radiation only emerges after it has multiply bounced round in the confined magnetic structure, during which some energy is lost by absorption to the ferrite material. In a region of a ferromagnetic resonance, the spectra of MDMs strongly depend on the geometry of a ferrite body. The most pronounced resonance characteristics one can observe are in a quasi-two-dimensional (2D) ferrite disk. The coupling between an electromagnetic field in a microwave cavity and MDM oscillations in a quasi-2D ferrite disk shows a regular multiresonance spectrum of a high-quality factor [15,16]. Recently, it was shown that small ferrite disks with MDM spectra behave as strong attractors for electromagnetic waves at resonance frequencies of MDM oscillations [17]. It was found that the regions of strong subwavelength localization of electromagnetic fields (subwavelength energy hot spots) appear because of the

topological properties of MDM oscillations—the power-flow eigenvortices [17–19]. Because of the MDM vortices, one has strong magnon-photon coupling in microwaves. Such coupled states can be specified as the MDM-vortex polaritons.

Topological properties of MDMs are originated from nonreciprocal phase behaviors on a lateral surface of a ferrite disk. A numerical analysis of classical complex-wave fields in a ferrite disk gives evidence for the Poynting-vector vortices and the field rotation inside a ferrite disk at frequencies corresponding to the MDM resonances [17–19]. The rotation angle of the polarization plane of electromagnetic fields, evident from numerical studies, is represented by a geometrical phase. Manifestation of a geometrical phase in wave dynamics of confined classical structures is well known. For example, the Berry phase for light appears in a twisted optical fiber in which the trajectory of the wave vector makes a closed loop. In this case, the polarization plane rotates during propagation, and the rotation angle is represented by a Berry phase [20]. Due to a Berry phase, one can observe a spin-orbit interaction in optics. In particular, it was shown that a spin-orbit interaction of photons results in the fine splitting of levels in a ring dielectric resonator, similar to that of electron levels in an atom [21]. In our case, the geometrical phase of electromagnetic fields appears due to space- and time-variant subwavelength (with respect to free-space electromagnetic fields) magnetization profiles of MDMs in a ferrite disk [22].

The purpose of this paper is to study the scattering of microwave electromagnetic fields from MDM-vortex polaritons. The geometrical phase plays a fundamental role in forming the coupled states of electromagnetic fields with MDM vortices. Because of the intrinsic symmetry breakings of the vortex characteristics, a small ferrite particle with a MDM spectrum behaves as a point singular region for electromagnetic waves. Based on a numerical analysis of classical complex-wave fields, we show that, due to the spin-orbit interaction, MDM resonances have frequency splits. For the split states, one has the localization or cloaking of electromagnetic fields. A definite-phase relationship between the incident electromagnetic wave and the microwave magnetization in the MDM particle results in asymmetry in the forward and backward scatterings of electromagnetic waves. The broken reflection symmetry is intimately related to intrinsic symmetry properties of MDMs in a quasi-2D ferrite disk. The hidden helical structure of MS-potential wave functions inside a ferrite disk gives evidence for a geometrical phase associated with the MS-wave dynamics [22,23]. From a spectral analysis of MS-potential wave functions in a quasi-2D ferrite disk, it follows that, due to special boundary conditions on a lateral surface of a ferrite disk, one has the Berry connection double-valued-function surface magnetic currents and fluxes of gauge electric fields. The MDM ferrite disk is characterized by eigenelectric moments (anapole moments) [22,23].

The paper is organized as follows. In Sec. II, we present topological textures of MDM-vortex polaritons obtained from the numerical simulation of a structure of a rectangular waveguide with an enclosed small ferrite disk. We analyze the scattering-matrix characteristics and give a detailed analysis of the fields for these MDM-vortex polaritons. Sec. III is devoted to an analytical consideration of the possible origin of MDM-vortex polaritons. We study the helicity and the orthogonality conditions of the MDMs in a ferrite disk and analyze properties of the observed split-state resonances. The paper is concluded with a summary in Sec. IV.

II. DISTINCT TOPOLOGICAL TEXTURES OF MDM-VORTEX POLARITONS

In one of the models, we can consider the fields associated with MDMs in a quasi-2D ferrite disk as the structures originated from rotating magnetic dipoles and rotating electric quadrupoles. Due to such field structures, one can observe the power-flow vortices inside a ferrite disk and in a near-field vacuum region [17–19]. Distinct topological textures of MDM-vortex polaritons become evident from numerical studies based on the HFSS electromagnetic simulation program (the software based on the finite-element method produced by ANSOFT Company). In a numerical analysis in the present paper, we use the same disk parameters as in Refs. [17–19]: The yttrium-iron-garnet (YIG) disk has a diameter of $D = 3$ mm, and the disk thickness is $t = 0.05$ mm; the disk is normally magnetized by a bias magnetic field $H_0 = 4900$ Oe; the saturation magnetization of a ferrite is $4\pi M_s = 1880$ G. Similar to Refs. [17–19], a ferrite disk is placed inside a TE_{10}-mode rectangular X-band waveguide in a position symmetrical to the waveguide walls and so that a disk axis is perpendicular to the wide wall of a waveguide. The waveguide walls are made of a perfect electric conductor (PEC). For better understanding of the field structures, we use a ferrite disk with a very small linewidth of $\Delta H = 0.1$ Oe. Figure 1 shows the module and phase-frequency characteristics of the reflection (the S_{11} scattering-matrix parameter) coefficient, whereas, Fig. 2 shows the module and phase-frequency characteristics of the transmission (the S_{21} scattering-matrix parameter) coefficient. The resonance modes are designated in succession by numbers $n = 1,2,3,....$ The inset in Fig. 1(a) shows the geometry of a structure: a ferrite disk enclosed in a rectangular waveguide.

The field structures of the MDM oscillations are very different from the field structures of the eigenmodes of an empty rectangular waveguide [17–19]. MDM-vortex polaritons appear as a result of the interaction of MDM oscillations with propagating electromagnetic waves. In the represented characteristics, one can clearly see that, starting from the second mode, the coupled states of the electromagnetic fields with MDM vortices are split-resonance states. In Fig. 1, these split resonances are denoted by single and double primes. The split resonances are characterized by two coalescent behaviors, namely, strong transmission and strong reflection of electromagnetic waves in a waveguide. In the case of the observed strong transmission (resonances denoted by a single prime), microwave excitation energy is transformed into MDM energy and is reemitted in the forward direction, whereas, in the case of strong reflection (resonances denoted by double primes), microwave excitation energy is transformed into MDM energy and is reemitted in the backward direction. As the most pronounced illustration of the MDM-vortex-polariton characteristics, we focus our paper on the second-mode ($n = 2$) coalescent resonances designated as $2'$ and $2''$ resonances. The

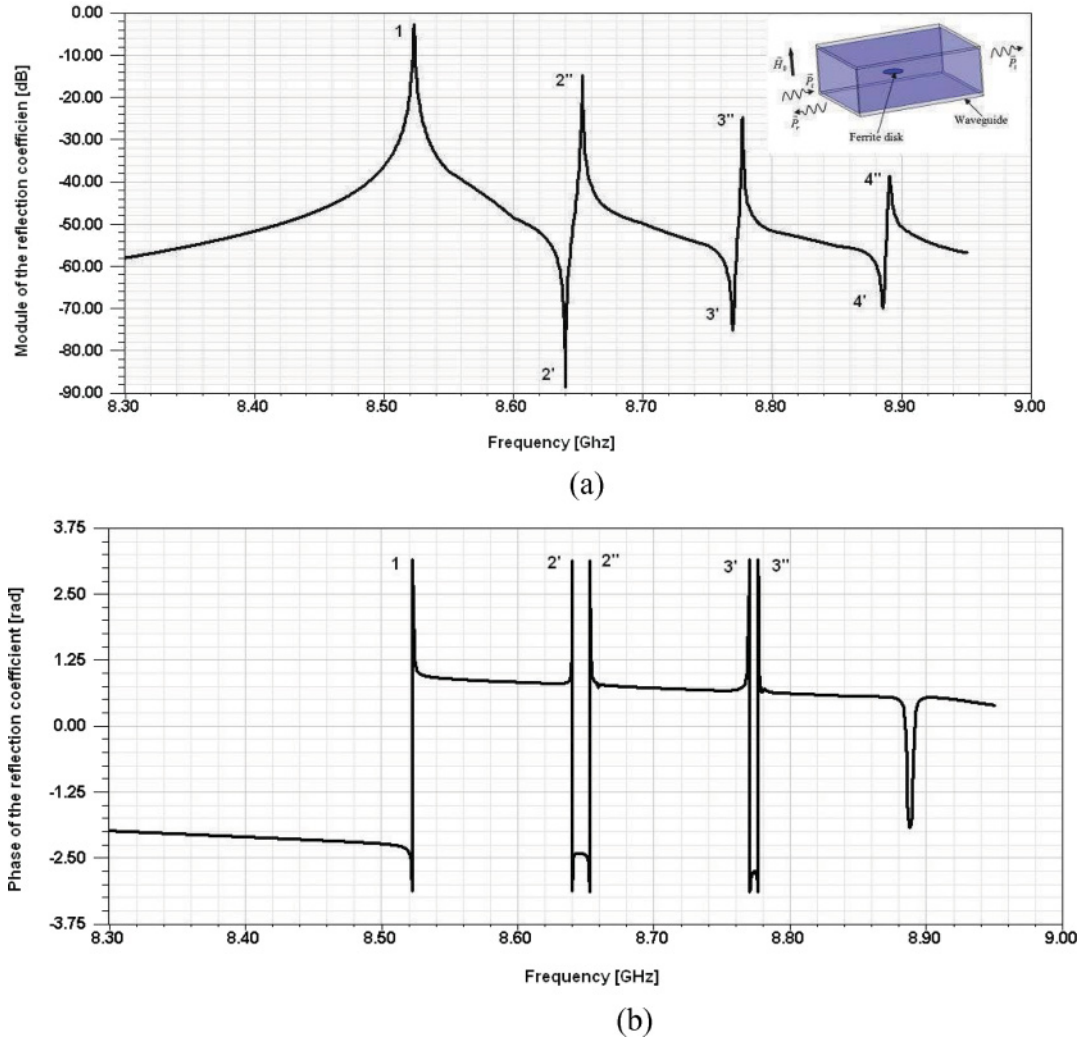

FIG. 1. (Color online) Frequency characteristics of (a) a module and (b) a phase of the reflection coefficient for a rectangular waveguide with an enclosed thin-film ferrite disk. The resonance modes are designated in succession by numbers $n = 1, 2, 3\ldots$. The coalescent resonances are denoted by single and double primes. The inset in (a) shows the geometry of a structure.

$2'$ resonance is the low-frequency resonance, while the $2''$ resonance is the high-frequency resonance. Figures 3 and 4 show the power-flow density distributions in a near-field vacuum region (a vacuum plane 75 μm above or below a ferrite disk) for the $2'$ and $2''$ resonances, respectively. One can see that, for the $2'$ resonance, there are two power-flow vortices of the near fields with opposite topological charges (positive for the counterclockwise vortex and negative for the clockwise vortex). Because of such a topological structure near a ferrite disk, a power flow in a waveguide effectively bends around a ferrite disk resulting in a negligibly small reflected wave. Evidently, at the $2'$-resonance frequency, one has electromagnetic-field transparency and cloaking for a ferrite particle. Contrary to the above behavior, at the $2''$-resonance frequency, there is a strong reflection of electromagnetic waves in a waveguide. The power-flow distribution above and below a ferrite disk is characterized by a single-vortex behavior with strong localization of an electromagnetic field. Such a resonance behavior (the $2''$ resonance) is known from our previous studies in Refs. [17–19]. Figures 5 and 6 show the electric-field distributions at two time phases ($\omega t = 0^\circ$ and $\omega t = 90^\circ$) in a vacuum region (75 μm above a ferrite disk) for the $2'$ and $2''$ resonances, respectively. Evidently, there is a rotational degree of freedom for the electric-field vectors resulting in a precession behavior of the electric field in vacuum.

For understanding the properties of the MDM-vortex polaritons, we should correlate the field structures in the near-field vacuum region and inside a ferrite disk. The power-flow density inside a ferrite disk for the $2'$ and $2''$ resonances are shown in Figs. 7(a) and 7(b), respectively. Figures 8 and 9 show the electric-field distributions at two time phases ($\omega t = 0^\circ$ and $\omega t = 90^\circ$) inside a ferrite disk for the $2'$ and $2''$ resonances, respectively. One can see that, despite some small differences in the pictures of the fields and power flows, the shown distributions inside a ferrite disk for the split-state $2'$ and $2''$ resonances are almost the same. They are the pictures typical for the second MDM in a ferrite disk [18,19]. At the same time, in vacuum, one has a strong difference between the near-field pictures for the $2'$ and $2''$ resonances (see Figs. 3–6).

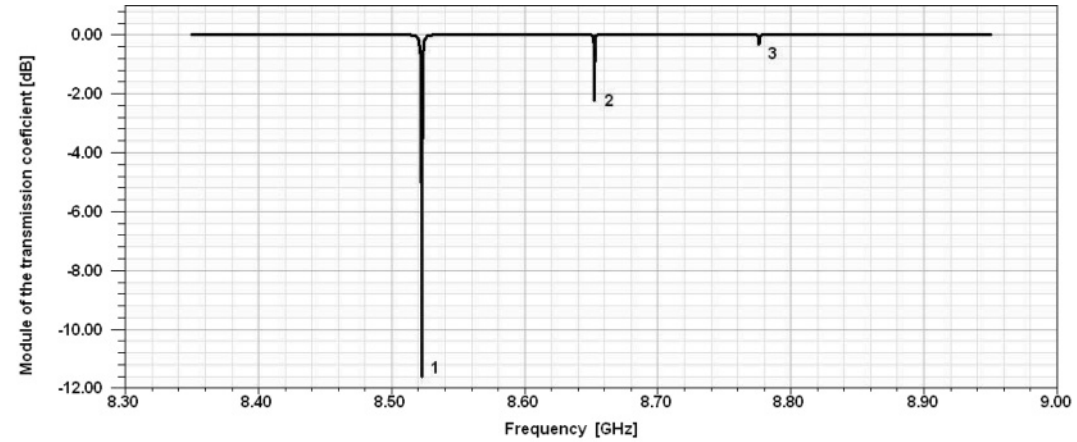

(a)

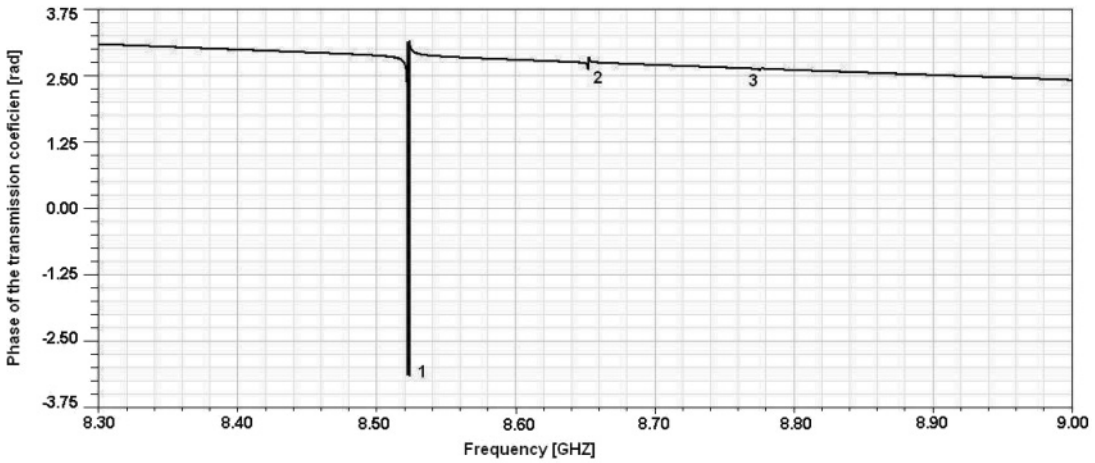

(b)

FIG. 2. Frequency characteristics of (a) a module and (b) a phase of the transmission coefficient for a rectangular waveguide with an enclosed thin-film ferrite disk. The resonance modes are designated in succession by numbers $n = 1, 2, 3\ldots$.

A distinctive feature of the electric-field structures, both inside and outside a ferrite disk, is the presence of the local circular polarization of electromagnetic waves together with a cyclic evaluation of the electric field around a disk axis. An explicit illustration of such evolutions of an electric field inside a disk is given in Fig. 10 in an assumption that the rotating-field vector has constant amplitude. One can see that the electric-field vectors are mutually parallel. When (for a given radius and at a certain time phase ωt) an azimuth angle θ varies from 0 to 2π, the electric-field vector accomplishes the geometric-phase rotation. This is the nonintegrable phase factor arising from a circular closed-path parallel transport of a system (an electric-field vector). We have wave plates continuously rotating locally and rotating along the power flow circulating around a disk axis. As we will show in the next section of the paper, the observed geometric-phase rotation of the electric-field vector is intimately related to hidden helical properties of MDMs. A disk axis can be considered as a line defect corresponding to adding or to subtracting an angle around a line. Such a line defect, in which rotational symmetry is violated, is an example of disclination. One can conclude that microwave fields of the MDM-vortex polaritons are characterized by spin and orbital angular momentums. The spin and orbital angular momentums, both oriented normally to a disk plane, are in the proper direction for the interaction. This results in resonance splittings in the MDM spectra. Our analysis indicates that the propagation of the waveguide-mode field is influenced by the spin-orbit interaction in a ferrite particle. Such a spin-orbit interaction plays the role of the vector potential for the waveguide-mode field. The waveguide mode travels through the substance of the whirling power flow and is deflected by the MDM-vortex vector potential. The waveguide field experiences the MDM power-flow vortex in the same way as a charged-particle wave experiences a vector potential Aharonov-Bohm effect. This is similar to the optical Aharonov-Bohm effect when light travels through the whirling liquid [24].

It is necessary to note, however, that there are some doubts as to whether spin and orbital angular momenta, in general, are separately physically observable. Maxwell's equations in vacuum are not invariant under spin and orbital angular momenta because of the transversality condition on the electromagnetic fields. They are invariant under the total (spin plus orbital) angular momentum operator. As a consequence, no photon

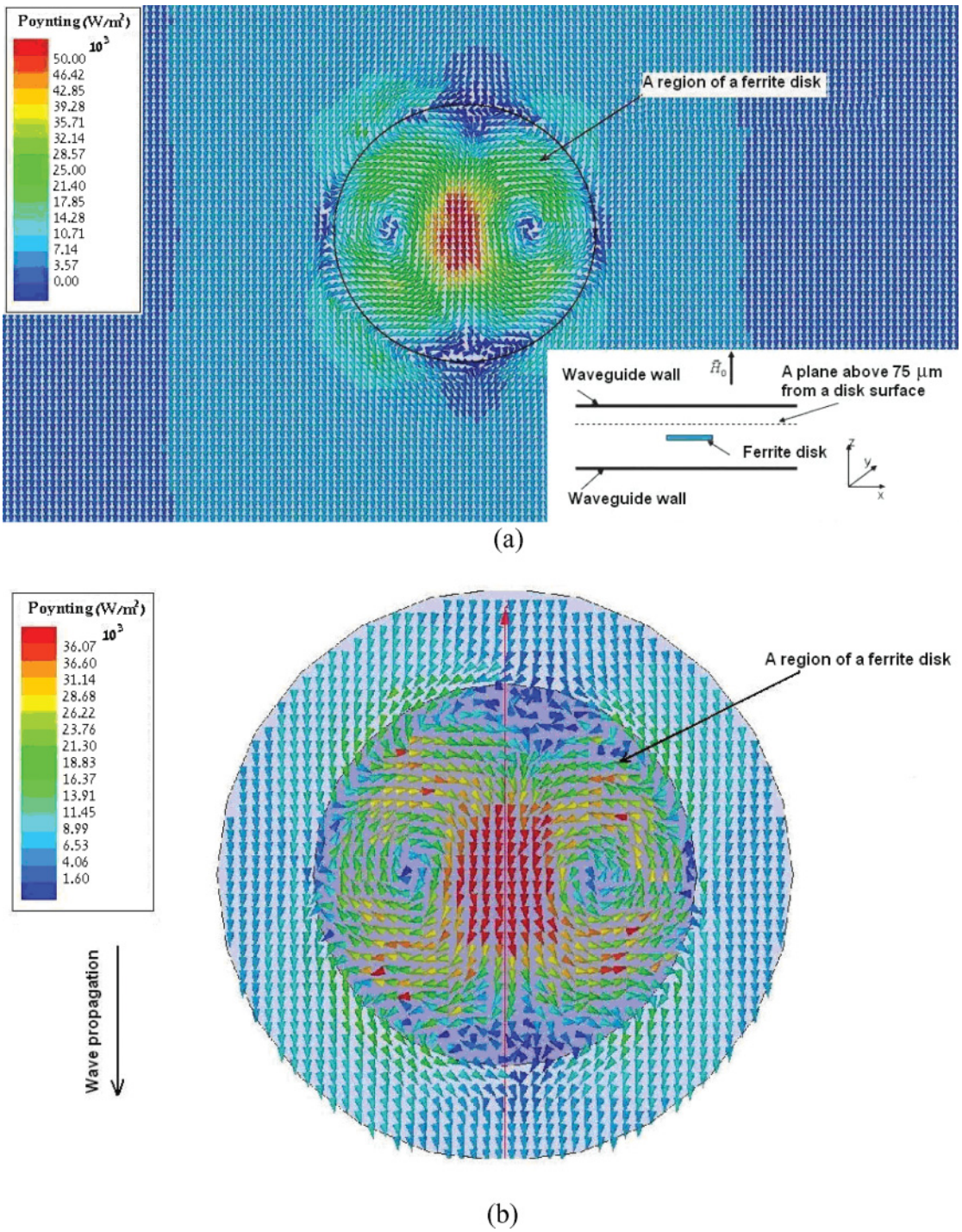

FIG. 3. (Color online) The power-flow density distributions in a near-field vacuum region (75 μm above a ferrite disk) for the $2'$ resonance ($f = 8.641$ GHz). (a) A general picture in a waveguide, (b) a detailed picture near the region of a ferrite disk. There is evidence for electromagnetic-field transparency and cloaking.

state exists with definite values of spin and orbital angular momenta. Here, it is relevant to make some comparison of our results to the properties of spin and orbital angular momenta of the fields in optical helical beams and optical near-field structures. In optics, it was shown that, besides the angular momentum related to photon spin, light beams in free space may also carry orbital angular momentum. Such beams are able to exert torques on matter [25]. For particles trapped on the beam axis, both spin and orbital angular momenta are transferred with the same efficiency so that the applied torque is proportional to the total angular momentum [26]. In literature, it is pointed out that the situation for understanding the physics of the spin and orbital angular momenta of light becomes more complicated in the optical near-field regime, where the optical fields, under the influence of the material environment, exhibit quite a different nature from those in free

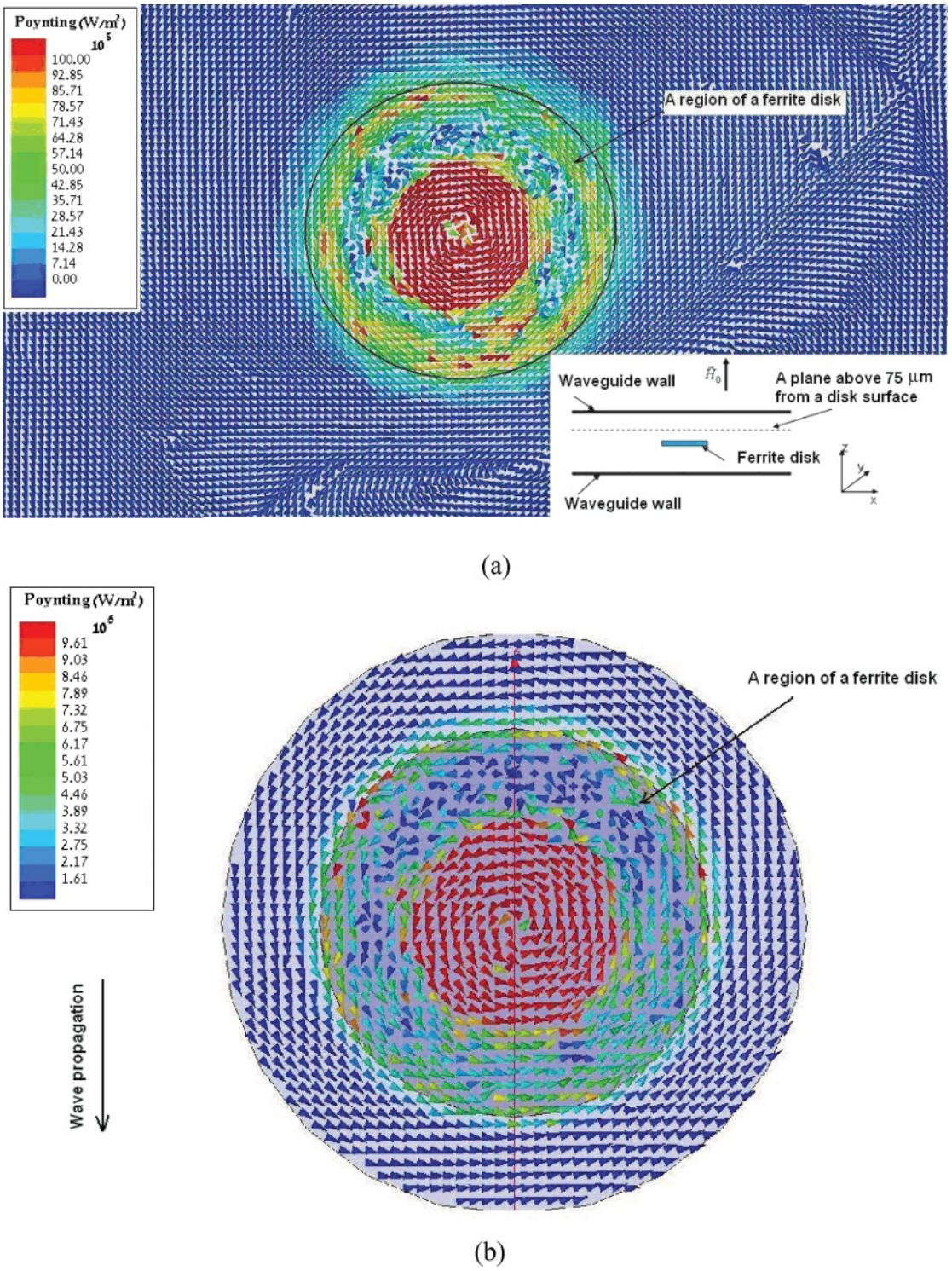

FIG. 4. (Color online) The power-flow density distributions in a near-field vacuum region (75 μm above a ferrite disk) for the 2″ resonance ($f = 8.652$ GHz). (a) A general picture in a waveguide, (b) a detailed picture near the region of a ferrite disk. One has strong localization and strong reflection of electromagnetic fields in a waveguide.

space. Reflecting the nature of coupled modes of optical fields and material excitations, the physical quantities associated with optical near-field interactions have distinctive properties in comparison to optical radiation in the far field [27]. These effects in optics can be useful for understanding the physics of the MDM-vortex polaritons in microwaves.

For a more detailed analysis of the field polarization in MDM-vortex polaritons, we insert a piece of metal wire inside a waveguide-vacuum region. A metal rod is made of a perfect electric conductor and has a very small size compared to the free-space electromagnetic wavelength: the diameter of 200 μm and the length of 1 mm. When such a small rod

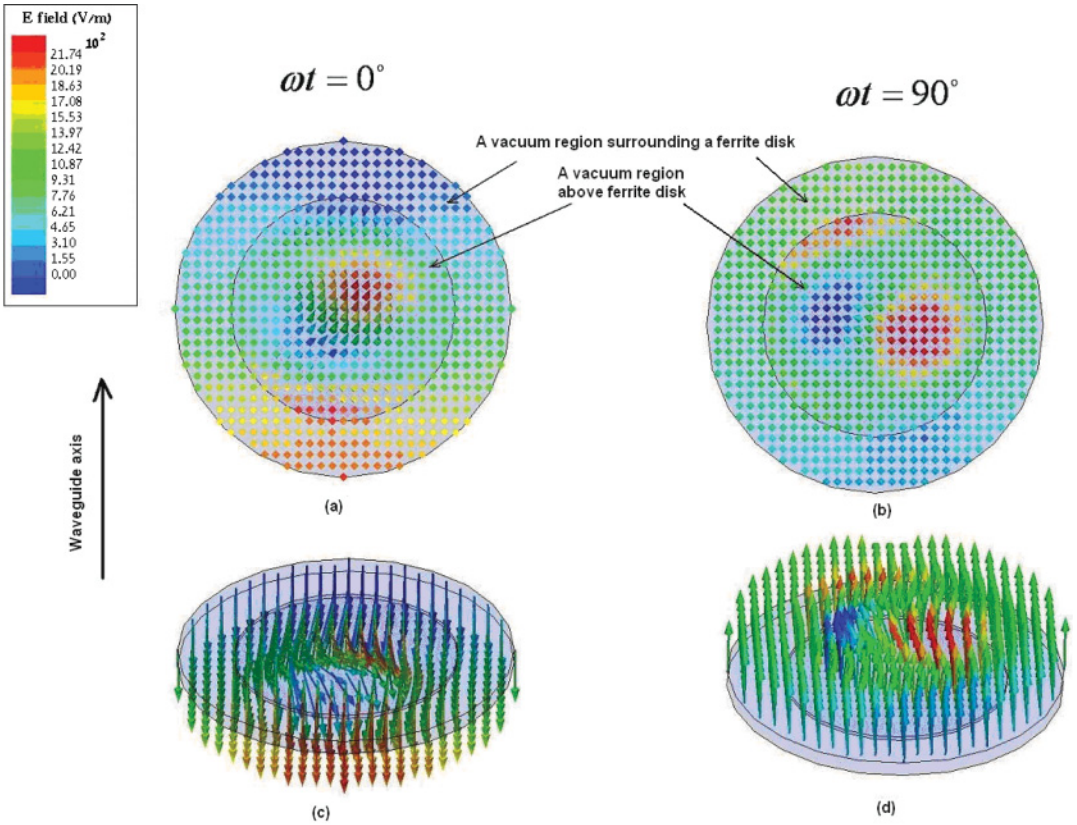

FIG. 5. (Color online) The electric-field distributions in a vacuum region (75 μm above a ferrite disk) for the $2'$ resonance at different time phases. (a) and (b) Top views, (c) and (d) side views.

is placed rather far from a ferrite disk and is oriented along an electric field of an empty rectangular waveguide, the field structure of an entire waveguide is not noticeably disturbed. At the same time, due to such a small rod, one can extract the fine structure of the fields at MDM resonances. Figures 11 and 12 show the electric fields on a small PEC rod for the $2'$ and $2''$ resonances, respectively. The rod position in a waveguide is shown in the inset in Fig. 11. The rod is placed along a disk axis. A gap between the lower end of the rod and the disk plane is 300 μm. From Fig. 11, it is evident that, for the $2'$ resonance (when one has electromagnetic-field transparency and cloaking), there is a trivial picture of the electric field induced on a small electric dipole inside a waveguide. At the same time, from Fig. 12, one sees that, in the case of the $2''$ resonance (when there is a strong reflection of electromagnetic waves in a waveguide), a PEC rod behaves as a small line defect on which rotational symmetry is violated. The observed evolution of the radial part of polarization gives evidence for the presence of a geometrical phase in the vacuum-region field of the MDM-vortex polariton.

In a general consideration, the model of MDM-vortex polaritons appears as an integrodifferential problem. Because of symmetry breakings, a MDM ferrite disk, being a very small particle compared to the free-space electromagnetic wavelength, is a singular point for electromagnetic fields in a waveguide. A topological character of such a singularity can be especially well illustrated by the structure of a magnetic field on a waveguide metallic wall for resonances characterized by strong reflection and localization of electromagnetic fields in a waveguide. In the spectral characteristics shown in Fig. 1, such resonances are designated by numbers 1, $2''$, $3''$, $4''$,.... For better representation, we will consider a resonance with the most pronounced field topology—the 1 resonance. Figure 13 shows a magnetic field on an upper wide wall of a waveguide for the 1 resonance at different time phases. One has to correlate this picture with a magnetic field, which is nearly a ferrite disk. Figure 14 shows a magnetic field in a vacuum region (75 μm above a ferrite disk) for the 1 resonance at different time phases. Since on the waveguide metal wall a magnetic field is purely planar (2D), the observed singularities are topological singularities of a magnetic field. Figure 13 clearly shows that a rotating planar magnetic field is characterized by the presence of surface topological magnetic charges (STMCs). The STMCs are points of divergence and convergence of a 2D magnetic field (or a surface magnetic flux density $\vec{B}_S$) on a waveguide wall. As is evident from Fig. 13, one has nonzero outward (inward) flows of a vector field $\vec{B}_S$ through a closed line C nearly surrounding points of divergence or convergence: $\oint_C \vec{B}_S \cdot \vec{n}_S dC \neq 0$. Here $\vec{n}_S$ is a normal vector to contour C, lying on a surface of a metal wall. At the same time, it is clear, however, that $\vec{\nabla}_S \cdot \vec{B}_S = 0$, since there is zero magnetic field at points of divergence or convergence. Topological singularities on the metal waveguide wall show unusual properties. One can see that, for the region bounded by the circle C, no planar variant of the divergence theorem takes place.

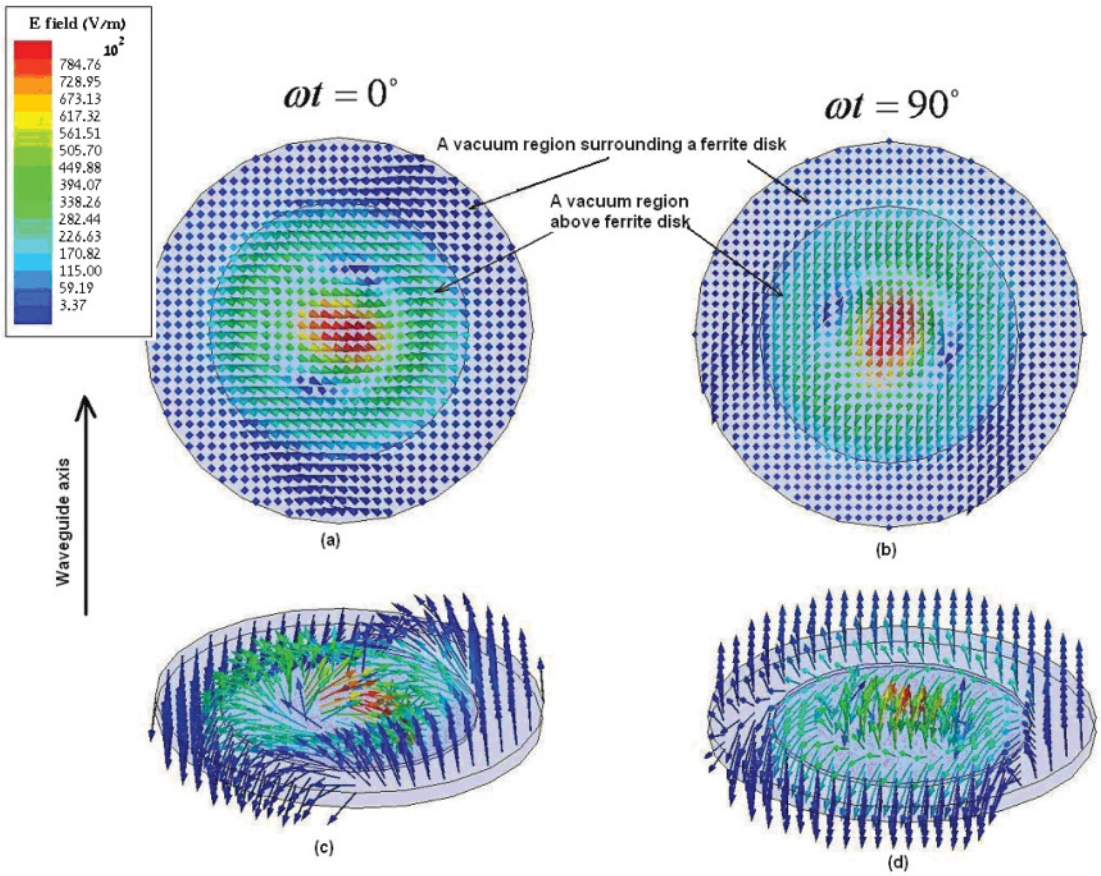

FIG. 6. (Color online) The electric-field distributions in a vacuum region (75 μm above a ferrite disk) for the $2''$ resonance at different time phases. (a) and (b) Top views, (c) and (d) side views.

III. THEORETICAL INSIGHT INTO THE ORIGIN OF THE MDM-VORTEX-POLARITON STRUCTURES

A nonintegrable electromagnetic problem of a ferrite disk in a rectangular waveguide, following from closed-loop nonreciprocal phase behavior on a lateral surface of a ferrite disk, can be solved numerically based on the HFSS program. From the above numerical analysis, we are able to conclude that, in a thin ferrite disk, microwave fields of MDM-vortex polaritons exhibit properties that can be characterized as originated from spin and orbital angular momenta. It can be supposed that, despite the fact that the spin and orbital angular momenta of the microwave fields are not separately observable, the shown split-resonance states of MDM-vortex polaritons are due to spin-orbit interactions. In general, however, numerical studies do not give us the ability for necessarily understanding the physics of the MDM-vortex polaritons. At the same time, a recently developed [22,23,28,29] analytical approach for MDM resonances based on a formulation of a spectral problem for a macroscopic scalar wave function—the MS-potential wave function ψ—may clarify physical properties of MDM-vortex polaritons. In this approach, the MDM dynamics is described magnetostatically: For time-varying fields, one neglects the electric displacement current in a Maxwell equation ($\vec{\nabla} \times \vec{H} = 0$). Spectral solutions for MS-potential wave functions ψ (which are introduced as $\vec{H} = -\vec{\nabla}\psi$) are obtained based on the Walker equation [11],

$$\vec{\nabla} \cdot (\overleftrightarrow{\mu} \cdot \vec{\nabla}\psi) = 0, \tag{1}$$

where $\overleftrightarrow{\mu}$ is a tensor of rf permeability. The analytical description of MDM oscillations in a quasi-2D ferrite particle rests on two cornerstones: (i) All precessing electrons in a magnetically ordered ferrite sample are described by a MS-potential wave function ψ, and (ii) the phase of this wave function is well defined over the whole ferrite-disk system, i.e., MDMs are quantumlike macroscopic states maintaining the global phase coherence. As shown in Refs. [17–19], the analytical ψ-function spectral characteristics are in good correspondence with the numerical HFSS spectra. In this section, we give a theoretical insight into the origin of the MDM-vortex-polariton structures based on studies of main symmetry and topological properties of MS-potential wave functions ψ in quasi-2D ferrite disks.

A. Helical resonances of MDMs in quasi-2D ferrite disks

The pictures of rotating (precessing) electric fields, shown in a previous section of the paper, give evidence for the left-right asymmetry of electromagnetic fields. The observed near-field photon helicity should be intimately related to hidden helical properties of MDMs. While the creation of a full-wave electromagnetic-field analysis of helicity in MDM-vortex polaritons entails great difficulties (because of nonintegrability, i.e., path dependence of the problem),

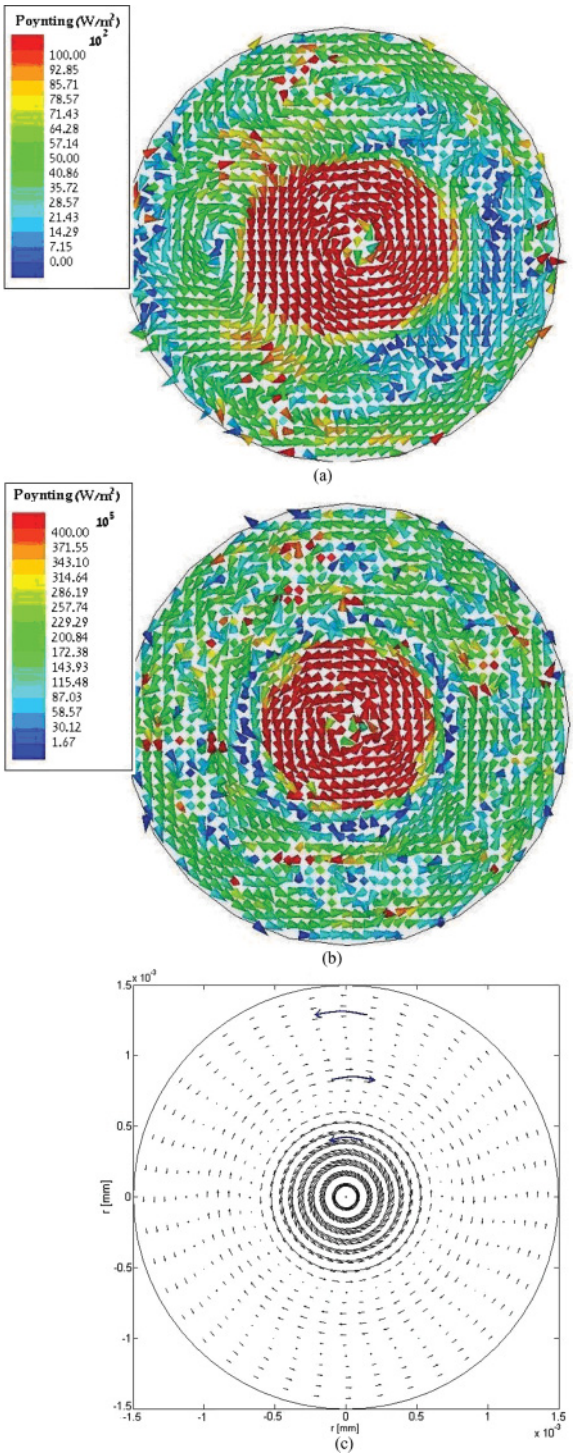

FIG. 7. (Color online) The power-flow density inside a ferrite disk. Numerically obtained vortices for (a) the $2'$ resonance and (b) the $2''$ resonance; (c) gives an analytical result for the second mode obtained from Eq. (11) for $\nu = 1$; big arrows clarify more precisely the directions of power flows.

analytical solutions of the ψ-function spectral problem can explain hidden helical properties of MDM resonances. Because of nonreciprocal phase behavior on a lateral surface of a ferrite disk, the phase variations for resonant ψ functions are both in azimuth θ and in axial z directions. This shows that proper spectral problem solutions for MDMs should be obtained in a helical-coordinate system. The helices are topologically nontrivial structures, and the phase relationships for waves propagating in such structures could be very special. Unlike the Cartesian- or cylindrical-coordinate systems, the helical-coordinate system is not orthogonal, and separating the right-handed and left-handed solutions is admitted. Since the helical coordinates are nonorthogonal and curvilinear, different types of helical-coordinate systems can be suggested. In our analysis of the MS-wave propagation, we use the Waldron helical-coordinate system [30].

In the Waldron coordinate system, the pitch of the helix is fixed, but the pitch angle is allowed to vary as a function of the radius. In cylindrical coordinates (r,θ,z), the reference surfaces, which are orthogonal, are given, respectively, by $r = \text{const}$, $\theta = \text{const}$, and $z = \text{const}$. In the Waldron helical system (r,ϕ,ζ), we retain the family of cylinders $r = \text{const}$ with meaning unchanged, but instead of the parallel planes $z = \text{const}$, we use a family of helical surfaces given by $z = \text{const} + p\theta/2\pi$ where p is the pitch. Figure 15 shows the helical reference surfaces $z = p\theta/2\pi$ for the (a) right-handed and (b) left-handed helical coordinates. Coordinate ζ is measured parallel to coordinate z from the reference surface $z = p\theta/2\pi$. The third coordinate surface is the set of planes $\theta = \text{const}$. We, however, use the azimuth coordinate ϕ instead of θ. Coordinate ϕ is numerically equal to coordinate θ, but whereas, θ is measured in a plane $z = \text{const}$, ϕ is measured in a helical surface $\zeta = \text{const}$. Let us consider a wave process in a helical structure with a constant pitch p. Geometrically, a certain phase of the wave can reach a point $(r,\theta,z+p)$ from the point (r,θ,z) in two independent ways. In the first way, due to translation in the ζ direction at $r = \text{const}$ and $\theta = \phi = \text{const}$, and, in the second way, due to translation in ϕ at $r = \text{const}$ and $\zeta = \text{const}$. In other words, for any point A with coordinates (r,ϕ,ζ), point B, being distant with a period of the helix, is characterized by coordinates $(r,\phi,\zeta+p)$ or by coordinates $(r,\phi+2\pi,\zeta)$. The regions between the surfaces $\zeta = np$ and $\zeta = (n+1)p$, for all integer numbers n, are continuous in a multiply connected space.

Let a dc magnetic field be directed along the z axis. In the Waldron helical system (r,ϕ,ζ), the Walker equation (1) takes the form [22,31]

$$\frac{\partial^2\psi}{\partial r^2} + \frac{1}{r}\frac{\partial\psi}{\partial r} + \frac{1}{r^2}\frac{\partial^2\psi}{\partial\phi^2} + \left(\frac{1}{\mu} + \tan^2\alpha_0\right)\frac{\partial^2\psi}{\partial\zeta^2} - 2\frac{1}{r}(\tan\alpha_0)^{(R,L)}\frac{\partial^2\psi}{\partial\phi\partial\zeta} = 0, \tag{2}$$

where superscripts R and L mean, respectively, right-handed and left-handed helical-coordinate systems and μ is a diagonal component of the permeability tensor. For pitch p, the pitch angles are defined from the relations,

$$(\tan\alpha_0)^{(R)} \equiv \tan\alpha_0 \equiv \bar{p}/r \quad \text{and}$$
$$(\tan\alpha_0)^{(L)} = -\tan\alpha_0 = -\bar{p}/r, \tag{3}$$

where $\bar{p} = p/2\pi$. The quantities $\tan\alpha_0$ and $\bar{p}$ are assumed to be positive. As shown in Refs. [22,31], for a given direction

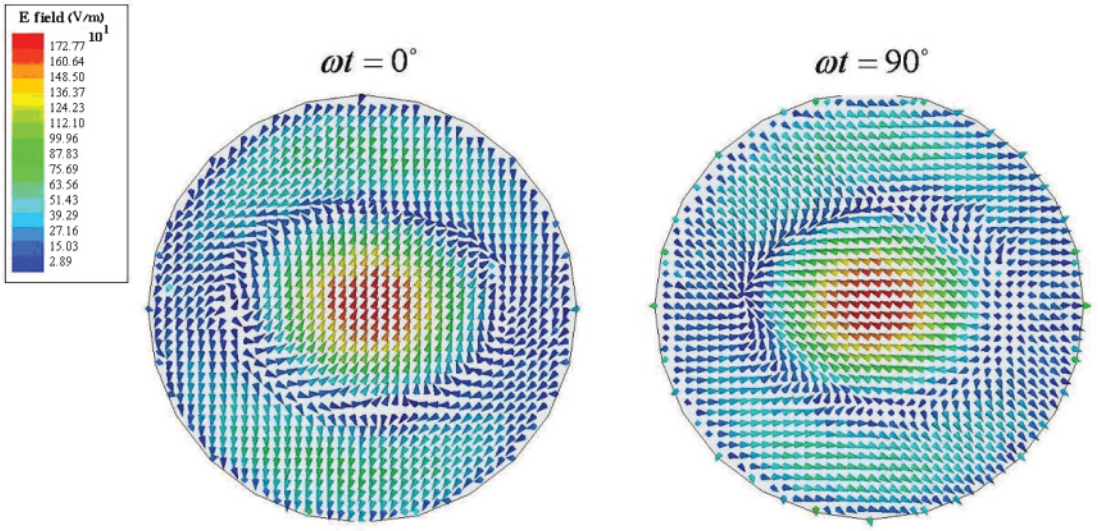

FIG. 8. (Color online) The electric-field distributions at different time phases inside a ferrite disk for the $2'$ resonance.

of a bias magnetic field, there are four types of helical modes. Inside a ferrite disk of radius $\Re$ ($r \leqslant \Re$), the solutions are in the form

$$\begin{aligned}
\psi^{(1)} &= a_1 J_{(w-\bar{p}\beta)}[(-\mu)^{1/2}\beta r]e^{-iw\phi}e^{-i\beta\zeta},\\
\psi^{(2)} &= a_2 J_{(w-\bar{p}\beta)}[(-\mu)^{1/2}\beta r]e^{+iw\phi}e^{-i\beta\zeta},\\
\psi^{(3)} &= a_3 J_{(w-\bar{p}\beta)}[(-\mu)^{1/2}\beta r]e^{+iw\phi}e^{+i\beta\zeta},\\
\psi^{(4)} &= a_4 J_{(w-\bar{p}\beta)}[(-\mu)^{1/2}\beta r]e^{-iw\phi}e^{+i\beta\zeta}.
\end{aligned} \tag{4}$$

For an outside region ($r \geqslant \Re$), one has

$$\begin{aligned}
\psi^{(1)} &= b_1 K_{(w-\bar{p}\beta)}(\beta r)e^{-iw\phi}e^{-i\beta\zeta},\\
\psi^{(2)} &= b_2 K_{(w-\bar{p}\beta)}(\beta r)e^{+iw\phi}e^{-i\beta\zeta},\\
\psi^{(3)} &= b_3 K_{(w-\bar{p}\beta)}(\beta r)e^{+iw\phi}e^{+i\beta\zeta},\\
\psi^{(4)} &= b_4 K_{(w-\bar{p}\beta)}(\beta r)e^{-iw\phi}e^{+i\beta\zeta}.
\end{aligned} \tag{5}$$

Here, w and β are wave numbers for the ϕ and ζ helical coordinates, respectively; J and K are Bessel functions of real and imaginary arguments, respectively. Coefficients $a_{1,2,3,4}$ and $b_{1,2,3,4}$ are amplitude coefficients. As an example, in Fig. 15, one can see the propagation directions of helical waves $\psi^{(1)}$ and $\psi^{(2)}$.

One of the most important properties of MDMs in a ferrite disk is the presence of helical-mode MS resonances [22,31]. For a given direction of a bias magnetic field (oriented along a disk axis), there exist two types of double-helix resonances in a quasi-2D ferrite disk. One resonance state is specified by the $\psi^{(1)} \leftrightarrow \psi^{(4)}$ phase correlation, when a closed-loop phase way is due to equalities for the wave numbers: $w^{(1)} = w^{(4)}$ and $\beta^{(1)} = \beta^{(4)}$. Another resonance state is specified by the $\psi^{(2)} \leftrightarrow \psi^{(3)}$ phase correlation with a closed-loop phase way due to equalities for the wave numbers: $w^{(2)} = w^{(3)}$ and $\beta^{(2)} = \beta^{(3)}$. The resonance $\psi^{(1)} \leftrightarrow \psi^{(4)}$, being

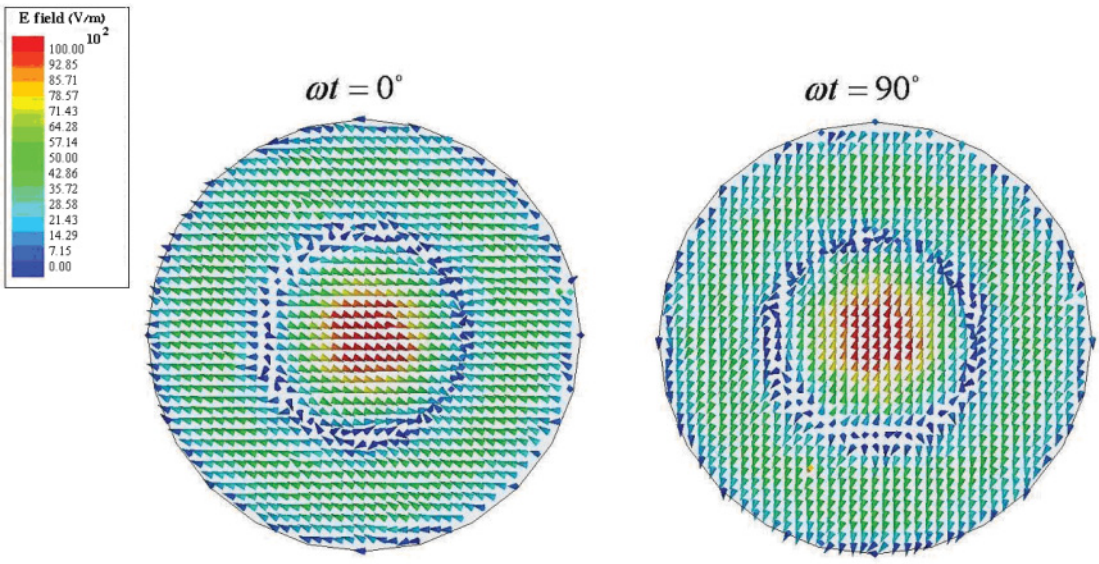

FIG. 9. (Color online) The electric-field distributions at different time phases inside a ferrite disk for the $2''$ resonance.

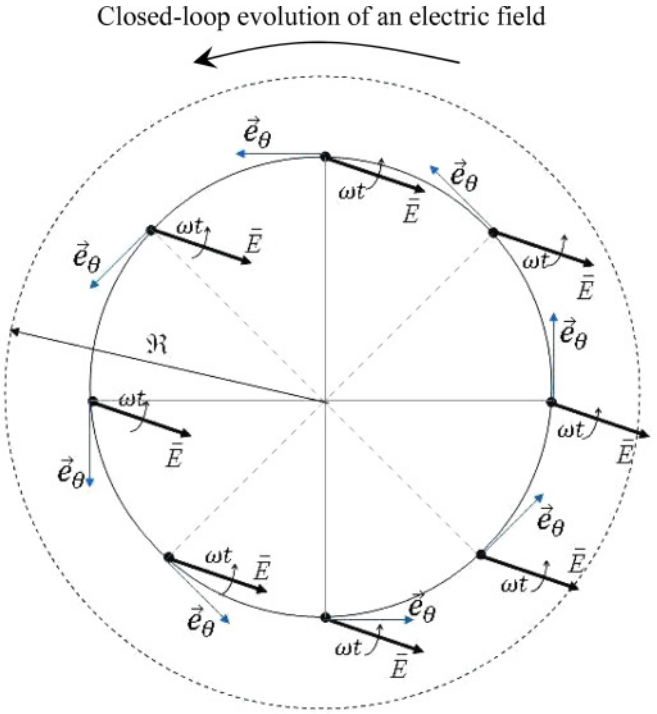

FIG. 10. (Color online) Explicit illustration of a cyclic evolution of an electric field inside a disk with the assumption that the rotating-field vector has constant amplitude. When (for a given radius and a certain time phase ωt) an azimuth angle θ varies from 0 to 2π, the electric-field vector accomplishes the geometric-phase rotation.

characterized by the right-hand rotation (with respect to a bias magnetic field directed along an axis of a disk, the z axis) of a composition of helices, is conventionally called the (+) resonance. The resonance $\psi^{(2)} \leftrightarrow \psi^{(3)}$, with the left-hand rotation of a helix composition, is conventionally called the (−) resonance. In a case of the (+) double-helix resonance, the azimuth phase overrunning the MS-potential wave functions is in correspondence with the right-hand resonance rotation of magnetization in a ferrite magnetized by a dc magnetic field directed along the z axis [11]. In Ref. [22], we discussed the question on experimental evidence for symmetry breaking of MDM oscillations caused by helical-mode resonances.

The helical-mode resonances of lossless magnetodipole oscillations in a ferrite disk are not characterized by the orthogonality relations. It can be shown that, for two helices giving a double-helix resonance in a ferrite disk, there are deferent power-flow densities [31]. Moreover, for such modes, there are no properties of parity ($\mathcal{P}$) and time-reversal ($\mathcal{T}$) invariance—the $\mathcal{PT}$ invariance. Solutions in Eqs. (4) and (5), being multiplied by a time factor $e^{i\omega t}$, describe propagating helical waves. Inversion of a direction of a bias magnetic field gives the inversion of time and so, the inversion of a sign of the off-diagonal component of the permeability tensor [11]. From an analysis in Ref. [22], one can see that, for the contrarily directed bias magnetic field, the (+) double-helix resonance appears due to the $\psi^{(2)} \leftrightarrow \psi^{(3)}$ phase-correlated helices, while the (−) double-helix resonance is due to the $\psi^{(1)} \leftrightarrow \psi^{(4)}$ interference. Such time inversion, however, cannot be accompanied by the space reflection with respect to a disk plane. Because of the lack of reflection symmetry for helical modes, there is no mutual reflection for helical modes $\psi^{(1)}$ and $\psi^{(3)}$ as well as no mutual reflection for helical modes $\psi^{(4)}$ and $\psi^{(2)}$. The $\mathcal{PT}$-symmetry breaking does not guarantee real-eigenvalue spectra, but, in the case of a lossless structure, can give spectra with pairs of complex-conjugate eigenvalues. It was shown, however, that by virtue of the quasi-2D of the problem, one can reduce solutions from helical to cylindrical coordinates with the proper separation of variables [22]. This gives integrable solutions for MDMs in a cylindrical-coordinate system. As we discuss below, such solutions can be considered as $\mathcal{PT}$ invariant. The $\mathcal{PT}$ -invariance properties of MDMs in a quasi-2D ferrite disk play an essential role in the physics of the observed topologically distinctive states.

B. $\mathcal{PT}$ -invariance properties of MDMs

As shown [19,22,23,28,29], for the (+) double-helix resonance, one can introduce the notion of an effective membrane function $\tilde{\varphi}$ and can describe the spectral problem in cylindrical coordinates by a differential-matrix equation,

$$(\hat{L}_\perp - i\beta\hat{R})\tilde{V} = 0, \tag{6}$$

where $\tilde{V} \equiv \begin{pmatrix} \tilde{\vec{B}} \\ \tilde{\varphi} \end{pmatrix}$, $\tilde{\varphi}$ is a dimensionless membrane MS-potential wave function and $\tilde{\vec{B}}$ is a dimensionless membrane function of a magnetic flux density. In Eq. (6), $\hat{L}_\perp$ is a differential-matrix operator,

$$\hat{L}_\perp \equiv \begin{pmatrix} (\overleftrightarrow{\mu}_\perp)^{-1} & \vec{\nabla}_\perp \\ -\vec{\nabla}_\perp \cdot & 0 \end{pmatrix}, \tag{7}$$

where subscript $\perp$ means correspondence with the in-plane r,θ coordinates, β is the MS-wave propagation constant along the z axis ($\psi = \tilde{\varphi}e^{-i\beta z}, \vec{B} = \tilde{\vec{B}}e^{-i\beta z}$), $\overleftrightarrow{\mu}$ is the permeability tensor, $\hat{R}$ is a matrix,

$$\hat{R} \equiv \begin{pmatrix} 0 & \vec{e}_z \\ -\vec{e}_z & 0 \end{pmatrix},$$

and $\vec{e}_z$ is a unit vector along the z axis. The boundary condition of the continuity of a radial component of the magnetic-flux density on a lateral surface of a ferrite disk of radius $\Re$ is expressed as [22,23,28]

$$\mu\left(\frac{\partial\tilde{\varphi}}{\partial r}\right)_{r=\Re^-} - \left(\frac{\partial\tilde{\varphi}}{\partial r}\right)_{r=\Re^+} = -i\frac{\mu_a}{\Re}\left(\frac{\partial\tilde{\varphi}}{\partial\theta}\right)_{r=\Re^-}, \tag{8}$$

where μ and μ_a, respectively, are diagonal and off-diagonal components of the permeability tensor $\overleftrightarrow{\mu}$. The modes described by a differential-matrix equation (6), are conventionally called L modes. With the use of separation of variables and boundary conditions of continuity of a MS-potential wave function and a magnetic-flux density on disk surfaces, one obtains solutions for the L modes. For a ferrite disk of radius $\Re$ and thickness d, there are the solutions [18,22]:

$$\psi(r,\theta,z,t) = C\xi(z)J_\nu\left(\frac{\beta r}{\sqrt{-\mu}}\right)e^{-i\nu\theta}e^{i\omega t}, \tag{9}$$

inside a ferrite disk ($r \leqslant \Re$, $-d/2 \leqslant z \leqslant d/2$) and

$$\psi(r,\theta,z,t) = C\xi(z)K_\nu(\beta r)e^{-i\nu\theta}e^{i\omega t}, \tag{10}$$

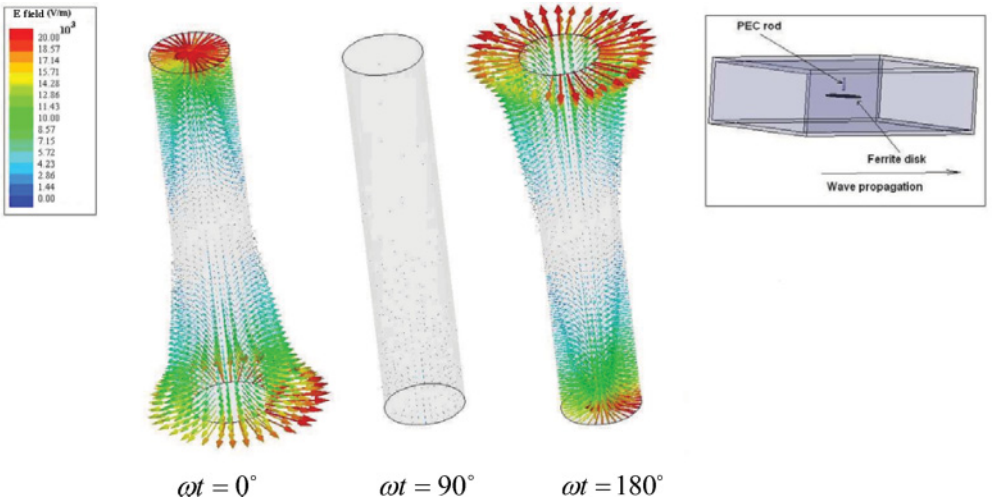

FIG. 11. (Color online) Electric field on a small PEC rod for the $2'$ resonance at different time phases. There is a trivial picture of the fields of a small electric dipole inside a waveguide. The inset shows the position of a PEC rod in a waveguide.

outside a ferrite disk (for $r \geqslant \Re$, $-d/2 \leqslant z \leqslant d/2$). In these equations, ν is an azimuth number, J_ν and K_ν are the Bessel functions of order ν for real and imaginary arguments, C is a dimensional coefficient, and $\xi(z)$ is an amplitude factor. For the solutions represented by Eqs. (9) and (10), the characteristic equation (8) takes the form

$$(-\mu)^{1/2}\left(\frac{J'_\nu}{J_\nu}\right)_{r=\Re} + \left(\frac{K'_\nu}{K_\nu}\right)_{r=\Re} - \frac{\nu\mu_a}{\beta\Re} = 0, \qquad (11)$$

where the prime denotes differentiation with respect to the argument. It is necessary to note that, in accordance with the (+) double-helix-resonance conditions [22], the azimuth number ν takes only integer and positive quantities. The membrane MS-potential functions $\tilde{\varphi}$ for the L modes do not have the standing-wave configuration in a disk plane but are azimuthally

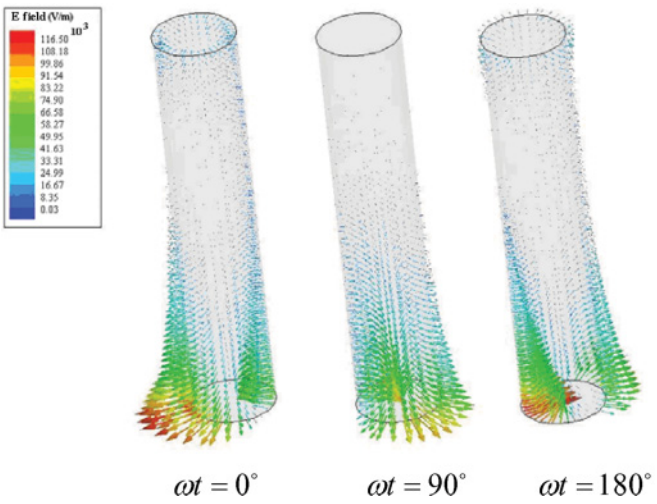

FIG. 12. (Color online) Electric field on a small PEC rod for the $2''$ resonance at different time phases. A PEC rod behaves as a small line defect on which rotational symmetry is violated. The observed evolution of the radial part of polarization gives evidence for the presence of a geometrical phase in the vacuum-region field of the MDM-vortex polariton.

propagating waves. For rotationally nonsymmetric waves, one has the azimuth power-flow density [18],

$$[p_q(r,z)]_\theta = \frac{\tilde{\varphi}_q^*(r)}{8\pi}\omega C_q^2[\xi_q(z)]^2\left[-\tilde{\varphi}_q(r)\frac{\mu}{r}\nu - \mu_a\frac{\partial\tilde{\varphi}_q(r)}{\partial r}\right]. \qquad (12)$$

Here, q is a number of radial variations (for a given azimuth number ν). Since an amplitude of a MS-potential function is equal to zero at $r = 0$, the power-flow density is zero at the disk center. Equation (12) describes the power-flow-density vortex inside a ferrite disk. For the second MDM, the circulating power-flow density was analytically calculated based on Eq. (12) and with the use of the disk parameters mentioned above for the HFSS simulation. Figure 7(c) shows the results of such a calculation for $\nu = +1$ and $q = 2$. One can see that this analytical representation is in good correlation with the numerical results of the power-flow densities inside a ferrite disk for the $2'$ and $2''$ resonances [see Figs. 7(a) and 7(b)].

The spectral-problem solutions for the L modes give real eigenvalues of propagation constants β and orthogonality conditions for eigenfunctions $\begin{pmatrix}\tilde{\vec{B}}\\ \tilde{\varphi}\end{pmatrix}$. For a certain mode n, the norm is defined as [18,19,23,28]

$$N_n = \int_S (\tilde{\varphi}_n\tilde{\vec{B}}_n^* - \tilde{\varphi}_n^*\tilde{\vec{B}}_n)\cdot\vec{e}_z dS, \qquad (13)$$

where S is the square of an open MS-wave cylindrical waveguide. The norm N_n, being multiplied by a proper dimensional coefficient, corresponds to the power-flow density of the MS-waveguide mode n through a MS-waveguide cross section. In an assumption of separation of variables in a cylindrical-coordinate system, this power-flow along the z axis should be considered independently of the azimuth power-flow density defined by Eq. (12). It follows, however, that because of special symmetry properties of the L modes (azimuthal nonsymmetry of membrane functions $\tilde{\varphi}$), representation of the norm by Eq. (13) is not so definite, and operator $\hat{L}_\perp$ cannot be considered as a self-adjoint operator. At the same time, as we

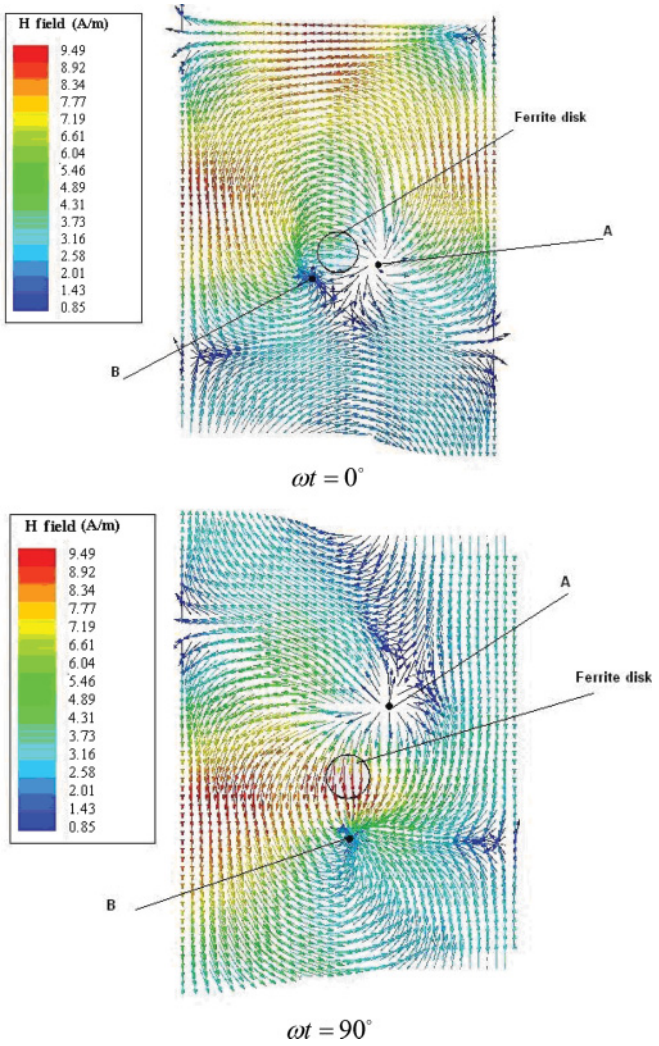

FIG. 13. (Color online) Magnetic field on a wide waveguide wall for the 1 resonance at different time phases. Points A and B, respectively, are positive and negative surface topological magnetic charges.

will show, operator $\hat{L}_\perp$ is $\mathcal{PT}$ invariant,

$$\hat{L}_\perp = (\hat{L}_\perp)^{\mathcal{PT}}. \tag{14}$$

This may presume the absence of complex eigenvalues for the L modes [32].

It is worth beginning our studies of the symmetry properties with some illustrative analyses of cylindrical-coordinate modes in a disk resonator. Let us consider, initially, a simple case of a nonmagnetic disk resonator. For resonance processes in a nonferrite dielectric resonator characterized by an oscillation period T, time shifts $t = 0 \to t = T$ and $t = T \to t = 0$ are formally equivalent since there is no chosen direction of time for the electron motion processes inside a dielectric material. When a resonator has cylindrical geometry, a counterclockwise rotating wave (RW) acquires the phase $\Phi = 2\pi k$ ($k = 1,2,3,...$) at the time shift $t = 0 \to t = T$ and at the time shift $t = T \to t = 0$, a clockwise RW acquires the same phase $\Phi = 2\pi k$. Since, in a cylindrically symmetric nonferrite resonator, dynamical behaviors are not distinguished by time inversion, a counterclockwise RW cannot be excited separately from a clockwise RW. Let us consider now a ferrite-disk resonator. Suppose that, for a given direction of a normal bias magnetic field H_0, there is a counterclockwise RW in a ferrite disk, and this wave acquires phase Φ_1 at the time shift $t = 0 \to t = T$, where T is an oscillation period. Performing time inversion (inversion of a direction of a bias magnetic field H_0), we obtain a clockwise RW. For this wave, we then consider the time shift $t = -T \to t = 0$. We suppose that, in this case, a clockwise RW acquires phase Φ_2. A system comes back to its initial state when both partial rotating processes (counterclockwise and clockwise RWs), with phases Φ_1 and Φ_2, are involved. Since, geometrically, a system is azimuthally symmetric, it is evident that $|\Phi_1| = |\Phi_2| \equiv \Phi$. A total minimal phase due to two RW processes should be equal to 2π. Generally, one has $|\Phi_1| + |\Phi_2| = 2\Phi = 2\pi k$ or $\Phi = k\pi$, where $k = 1,2,3,....$ The phases for RWs in a MS-mode cylindrical resonator are shown in Fig. 16. To bring a system to its initial state, one should involve the time-reversal operations. When only one direction of a normal bias magnetic field is given and quantities k are odd integers, the MS wave rotating in a certain azimuth direction (either counterclockwise or clockwise) should make two rotations around a disk axis to come back to its initial state. It means that, for a given direction of a bias magnetic field and for odd integer k, a membrane function $\tilde{\varphi}$ behaves as a double-valued function.

It is worth noting that, in general, the phase of the final state differs from that of the initial state by

$$\Phi = \Phi_d + \Phi_g, \tag{15}$$

where Φ_d and Φ_g are the dynamical and geometric phases, respectively. If only the topology of the path is altered, then only $\Phi_g$varies [33]. In our case, this fact is illustrated very clearly by Figs. 8 and 9. Let us compare the positions of electric field vectors in Figs. 8 and 9 for a certain dynamical phase $\omega t = 0°$, for example. One can see that these vectors are shifted in space at an angle of 90°. At the same time, since the frequency shift between the $2'$ and $2''$ resonances is negligibly small ($\Delta f/f \approx 13/8645 = 0.0015$), the dynamical phase ($\omega t = 0°$) is the same. The observed strong variation of a geometric phase against the background on a nonvarying dynamical phase is a good confirmation of a topological character of the split-resonance states.

Now, let us analyze properties of operator $\hat{L}_\perp$. Following a standard way of solving boundary problems in mathematical physics [34,35], one can consider two joint boundary problems: the main boundary problem and the conjugate boundary problem. Both problems are described by differential equations that are similar to Eq. (6). The main boundary problem is expressed by the differential equation $(\hat{L}_\perp - i\beta\hat{R})\tilde{V} = 0$, and the conjugate boundary problem is expressed by the equation, $(\hat{L}^\circ_\perp - i\beta^\circ\hat{R}\,)\tilde{V}^\circ = 0$. From a formal point of view, initially, it is supposed that these are different equations: There are different differential operators, different eigenfunctions, and different eigenvalues. A form of differential operator $\hat{L}^\circ_\perp$ can be found from integration by parts,

$$\int_S (\hat{L}_\perp \tilde{V})(\tilde{V}^\circ)^* dS = \int_S \tilde{V}(\hat{L}^\circ_\perp \tilde{V}^\circ)^* dS + \oint_{\mathcal{L}} P(\tilde{V}, \tilde{V}^\circ) d\ell, \tag{16}$$

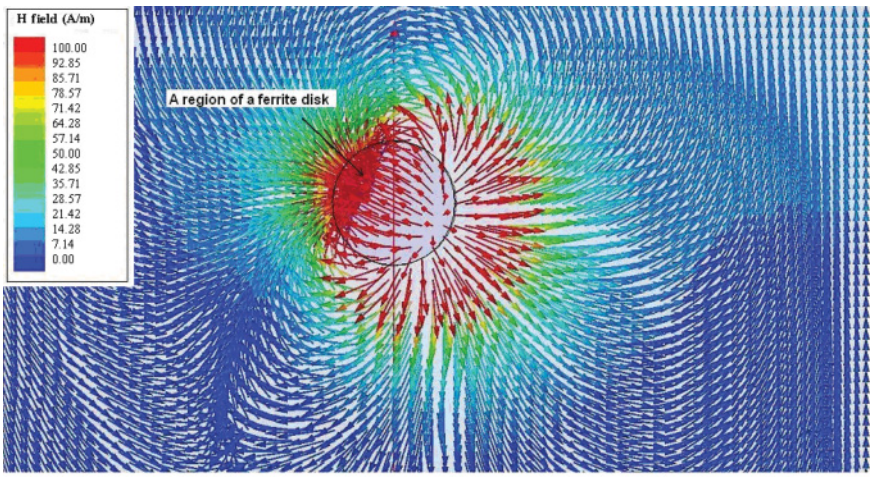

$\omega t = 0^\circ$

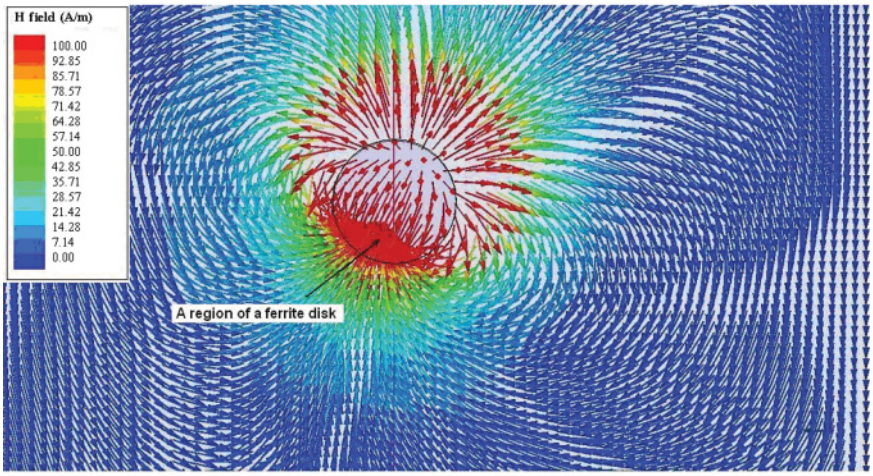

$\omega t = 90^\circ$

FIG. 14. (Color online) Magnetic field in a vacuum region (75 μm above a ferrite disk) for the 1 resonance at different time phases.

where $\mathcal{L} = 2\pi\Re$ is a contour surrounding a cylindrical ferrite core and $P(\tilde{V}, \tilde{V}^\circ)$ is a bilinear form. Operator $\hat{L}_\perp$ can be considered a self-adjoint (Hermitian) operator when permeability tensor $\ddot{\mu}$ is a Hermitian tensor, functions $\tilde{V}$ and $\tilde{V}^\circ$ are two mutually complex-conjugate functions, and the contour integral in the right-hand side of Eq. (16) is equal to zero [34,35]. The last condition means that, for an open ferrite structure [a core ferrite region (F) is surrounded by a dielectric region (D)], there are homogeneous boundary conditions for functions $\tilde{V}$ and $\tilde{V}^\circ$,

$$\oint_{\mathcal{L}} P(\tilde{V}, \tilde{V}^\circ) d\ell \equiv \oint_{\mathcal{L}} [P^{(F)}(\tilde{V}, \tilde{V}^\circ) + P^{(D)}(\tilde{V}, \tilde{V}^\circ)] d\ell = 0. \tag{17}$$

As we will show, in a general case, $\tilde{V}$ and $(\tilde{V}^\circ)^*$ are not two mutually complex-conjugate functions, and so, we do not have self-adjointness of operator $\hat{L}_\perp$. At the same time, there exist necessary conditions for the $\mathcal{PT}$ -invariant homogeneous boundary conditions (17) resulting in the $\mathcal{PT}$ invariance of operator $\hat{L}_\perp$.

For the contour integral on the right-hand side of Eq. (16), we have [23]

$$\oint_{\mathcal{L}} P(\tilde{V}, \tilde{V}^\circ) d\ell = -\oint_{\mathcal{L}} M(\tilde{V}, \tilde{V}^\circ) d\ell - \oint_{\mathcal{L}} N(\tilde{V}, \tilde{V}^\circ) d\ell, \tag{18}$$

where

$$\oint_{\mathcal{L}} M(\tilde{V}, \tilde{V}^\circ) d\ell \equiv \oint_{\mathcal{L}} \left\{ \left[\mu \left(\frac{\partial \tilde{\varphi}}{\partial r} \right)_{r=\Re^-} - \left(\frac{\partial \tilde{\varphi}}{\partial r} \right)_{r=\Re^+} \right] (\tilde{\varphi}^\circ)^*_{r=\Re} - (\tilde{\varphi})_{r=\Re} \left[\mu \left(\frac{\partial \tilde{\varphi}^\circ}{\partial r} \right)_{r=\Re^-} - \left(\frac{\partial \tilde{\varphi}^\circ}{\partial r} \right)_{r=\Re^+} \right]^* \right\} d\ell, \tag{19}$$

and

$$\oint_{\mathcal{L}} N(\tilde{V}, \tilde{V}^\circ) d\ell \equiv \frac{1}{\Re} \oint_{\mathcal{L}} \left\{ \left(i\mu_a \frac{\partial \tilde{\varphi}}{\partial \theta} \right) (\tilde{\varphi}^\circ)^* - (\tilde{\varphi}) \left[\left(i\mu_a \frac{\partial \tilde{\varphi}}{\partial \theta} \right)^\circ \right]^* \right\}_{r=\Re} d\ell. \tag{20}$$

In these equations, we used expressions for radial components of the magnetic-flux density: (a) for the main boundary problem, $\tilde{B}_r = -(\mu \frac{\partial \tilde{\varphi}}{\partial r} + i\mu_a \frac{1}{\Re} \frac{\partial \tilde{\varphi}}{\partial \theta})$ in a ferrite region and $\tilde{B}_r = -\frac{\partial \tilde{\varphi}}{\partial r}$ in a dielectric and (b) for the conjugate boundary problem, $\tilde{B}^\circ_r = -[\mu \frac{\partial \tilde{\varphi}^\circ}{\partial r} + (i\mu_a \frac{1}{\Re} \frac{\partial \tilde{\varphi}}{\partial \theta})^\circ]$ in a ferrite region and $\tilde{B}^\circ_r = -\frac{\partial \tilde{\varphi}^\circ}{\partial r}$ in a dielectric.

Following Eq. (15), we represent $\tilde{\varphi}$ and $\tilde{\varphi}^\circ$ as

$$\tilde{\varphi} \equiv \delta \tilde{\eta}, \tag{21}$$

$$\tilde{\varphi}^\circ \equiv \delta^\circ \tilde{\eta}^\circ. \tag{22}$$

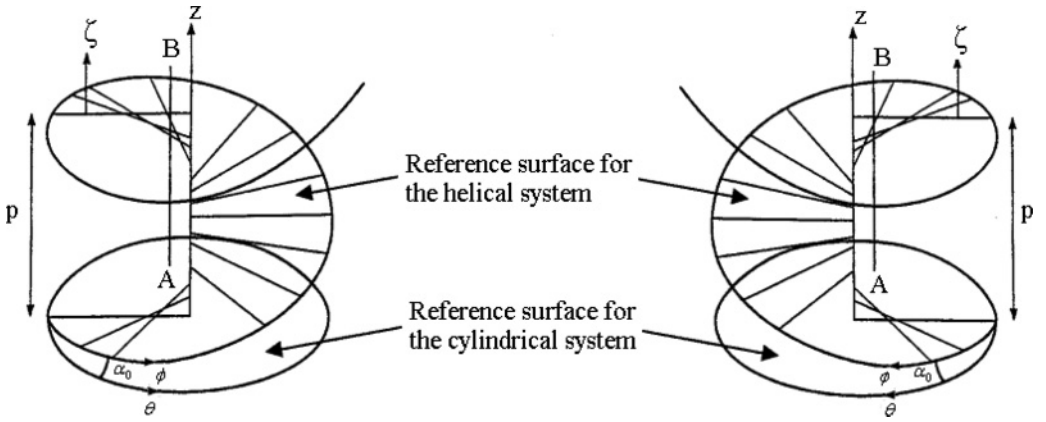

FIG. 15. (a) The right-handed and (b) the left-handed Waldron helical-coordinate systems. Coordinate ζ is measured parallel to coordinate z from the reference surface $z = p\theta/2\pi$. As an example, the arrows illustrate the propagation directions of helical waves: (a) wave $\psi^{(1)}$ and (b) wave $\psi^{(2)}$.

Functions $\tilde{\eta} \sim \tilde{e}^{-i\vartheta_d}$ and $\tilde{\eta}^\circ \sim \tilde{e}^{-i\vartheta_d^\circ}$ are characterized by dynamical phases ϑ_d and ϑ_d°, respectively, while functions $\tilde{\delta} \sim \tilde{e}^{-i\vartheta_g}$ and $\tilde{\delta}^\circ \sim \tilde{e}^{-i\vartheta_g^\circ}$ are characterized by geometrical phases ϑ_g and ϑ_g°, respectively. Evidently, the double valuedness of functions $\tilde{\varphi}$ and $\tilde{\varphi}^\circ$ is due to the presence of geometrical phases. It means that functions $\tilde{\eta}$ and $\tilde{\eta}^\circ$ are single-valued functions while functions $\tilde{\delta}$ and $\tilde{\delta}^\circ$ are double-valued functions. With such a representation, we can also say that functions $\tilde{\eta}$ and $\tilde{\eta}^\circ$ are described by orbital coordinates, whereas, functions $\tilde{\delta}$ and $\tilde{\delta}^\circ$ are described by spinning coordinates. Since $\tilde{\eta}$ and $\tilde{\eta}^\circ$ are space-reversally invariant, functions $\tilde{\eta}$ and $(\tilde{\eta}^\circ)^*$ can be considered just as complex-conjugate functions. At the same time, $\tilde{\delta}$ and $(\tilde{\delta}^\circ)^*$ are not complex-conjugate functions.

To satisfy homogeneous boundary relation (17), we consider conditions when both $\oint_{\mathcal{L}} M(\tilde{V}, \tilde{V}^\circ)d\ell$ and $\oint_{\mathcal{L}} N(\tilde{V}, \tilde{V}^\circ)d\ell$ are equal to zero. For integral $\oint_{\mathcal{L}} N(\tilde{V}, \tilde{V}^\circ)d\ell$, expressed by Eq. (20), there is the possibility to analyze the orthogonality conditions separately for the orbital coordinates and spinning coordinates [23,36]. The orbital-coordinate integral takes the form

$$\frac{1}{\Re}\oint_{\mathcal{L}}\left\{\left(i\mu_a\frac{\partial\tilde{\eta}}{\partial\theta}\right)(\tilde{\eta}^\circ)^* - (\tilde{\eta})\left[\left(i\mu_a\frac{\partial\tilde{\eta}}{\partial\theta}\right)^\circ\right]^*\right\}_{r=\Re} d\ell, \tag{23}$$

and the spinning-coordinate integral is expressed as

$$\frac{1}{\Re}\oint_{\mathcal{L}}\left\{\left(i\mu_a\frac{\partial\tilde{\delta}}{\partial\theta}\right)(\tilde{\delta}^\circ)^* - (\tilde{\delta})\left[\left(i\mu_a\frac{\partial\tilde{\delta}}{\partial\theta}\right)^\circ\right]^*\right\}_{r=\Re} d\ell. \tag{24}$$

For integral (23), one has

$$\oint_{\mathcal{L}}\left\{\left(i\mu_a\frac{\partial\tilde{\eta}}{\partial\theta}\right)(\tilde{\eta}^\circ)^* - (\tilde{\eta})\left[\left(i\mu_a\frac{\partial\tilde{\eta}}{\partial\theta}\right)^\circ\right]^*\right\}_{r=\Re} d\ell$$
$$= \oint_{\mathcal{L}}\left[\left(i\mu_a\frac{\partial\tilde{\eta}}{\partial\theta}\right)\tilde{\eta}^* - (\tilde{\eta})\left(i\mu_a\frac{\partial\tilde{\eta}}{\partial\theta}\right)^*\right]_{r=\Re} d\ell \equiv 0. \tag{25}$$

At the same time, one cannot just have integral (24) equal to zero only with time inversion. Function $\tilde{\delta}^\circ$ is considered as the $\mathcal{P}$-transformed function with respect to function $\tilde{\delta}$, and to have integral (24) equal to zero, one has to consider the combined $\mathcal{PT}$ transformation. It is evident that, in a quasi-2D ferrite-disk structure, geometrical-phase circular running waves $\tilde{\delta}$ will have an opposite direction of rotation for the z-axis reflection, so $\mathcal{P}$ is classified as a space reflection with respect to the z axis. When one considers waves $(\tilde{\delta}^\circ)^*$ as the waves, which are $\mathcal{PT}$ transformed relative to waves $\tilde{\delta}$, one has integral (24) equal to zero. In general, $(\tilde{\varphi}^\circ)^*$ is considered as a $\mathcal{PT}$-transformed function relative to $\tilde{\varphi}$. Because of the $\mathcal{PT}$ invariance of function $\tilde{\varphi}$, one concludes that integral (19) is identically equal to zero. As a result, one has zero integral (18).

An introduction of membrane functions in a quasi-2D ferrite-disk structure allows reducing the problem of parity transformation to a one-dimensional reflection in space. The geometrical-phase circular running of membrane function $\tilde{\varphi}$ will have an opposite direction of rotation for the z-axis reflection. From the above analysis of the contour integral $\oint_{\mathcal{L}} P(\tilde{V}, \tilde{V}^\circ)d\ell$, it follows that the study of the $\mathcal{PT}$ invariance of operator $\hat{L}_\perp$ with eigenfunctions $\begin{pmatrix}\tilde{\vec{B}}\\ \tilde{\varphi}\end{pmatrix}$ can be reduced to an

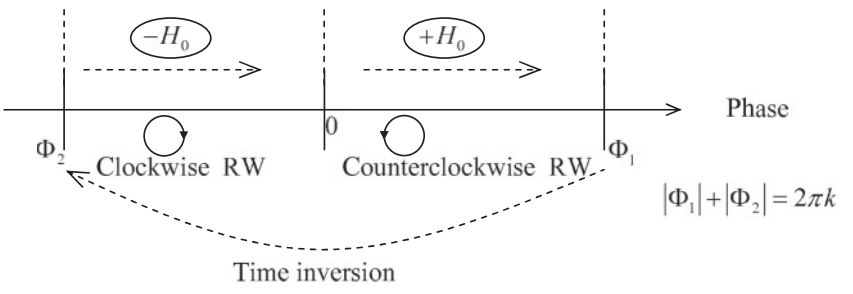

FIG. 16. The phases for Counterclockwise and Clockwise RWs in a MS-mode cylindrical resonator.

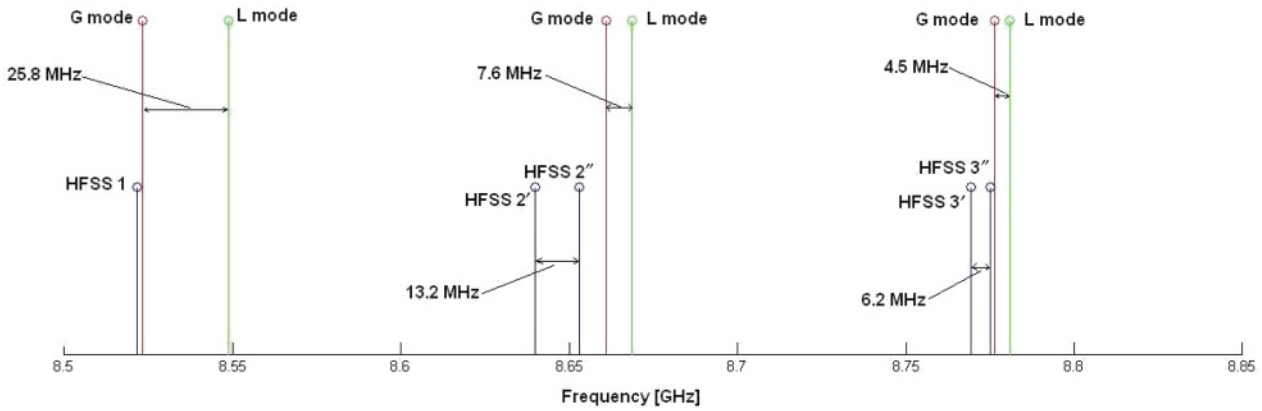

FIG. 17. (Color online) The spectrum peak positions for the HFSS simulation and the analytical L and G modes. Frequency differences for the peak positions of the analytically derived L and G modes are at the same order of magnitude as the frequency differences for the split-resonance states observed in the HFSS spectrum.

analysis of $\mathcal{PT}$ properties of membrane functions $\tilde{\varphi}$ on a lateral surface of a ferrite disk. Certainly, only the equation for boundary conditions reflects a nonreciprocal phase behavior and so, the path dependence of the boundary-value problem. It is clear that the simultaneous change of a sign of μ_a (the time reversal) and a sign of derivative $(\frac{\partial\tilde{\varphi}}{\partial\theta})_{r=\Re^-}$ (the space reflection) on the right-hand side of Eq. (8) leaves this equation invariable. This is evidence for the $\mathcal{PT}$ invariance. For a value of a MS-potential wave function on a lateral surface of a ferrite disk $\tilde{\varphi}|_{r=\Re}$, we can write

$$\mathcal{PT}\tilde{\varphi}|_{r=\Re}(z) = \tilde{\varphi}^*|_{r=\Re}(-z) = \tilde{\varphi}|_{r=\Re}(z). \tag{26}$$

There is also the possibility to introduce the orthogonality relation for two modes,

$$\begin{aligned}(\tilde{\varphi}_p|_{r=\Re},\tilde{\varphi}_q|_{r=\Re}) &= \oint_{\mathcal{L}} [\tilde{\varphi}_p|_{r=\Re}(z)]\tilde{\varphi}_q^*|_{r=\Re}(-z)d\ell \\ &= \oint_{\mathcal{L}} [\tilde{\varphi}_q|_{r=\Re}(z)][\mathcal{PT}\tilde{\varphi}_p|_{r=\Re}]d\ell. \end{aligned}\tag{27}$$

Here, we assume that the spectrum under consideration is real, and contour $\mathcal{L}$ is a real line. This orthogonality relation has different meanings for even and odd quantities k in equation for a phase of the rotating wave: $\Phi = k\pi$. For even quantities k, the edge waves show reciprocal phase behavior for propagation in both azimuthal directions. Contrarily, for odd quantities k, the edge waves propagate only in one direction of the azimuth coordinate. In the case of even k, the orthogonality relation (27) can be written as $(\tilde{\varphi}_p|_{r=\Re},\tilde{\varphi}_q|_{r=\Re}) = \delta_{pq}$, where δ_{mn} is the Kronecker delta. With respect to this relation, for odd k, one has $(\tilde{\varphi}_p|_{r=\Re},\tilde{\varphi}_q|_{r=\Re}) = -\delta_{pq}$. In a general form, the inner product (27) can be written as

$$(\tilde{\varphi}_p|_{r=\Re},\tilde{\varphi}_q|_{r=\Re}) = (-1)^k\delta_{pq}. \tag{28}$$

C. Hermiticity conditions for MDMs

We are faced with the fact that, in the bound states for functions $\tilde{\varphi}|_{r=\Re}$, there are equal numbers of positive-norm and negative-norm states. To some extent, our results resemble the results of the $\mathcal{PT}$-symmetry studies in quantum mechanics structures with a complex Hamiltonian [32,37,38]. Similar to the paper in Ref. [32], we can introduce a certain operator $\hat{\mathcal{C}}$, which is the observable that represents the measurement of the signature of the $\mathcal{PT}$ norm of a state. While, in the problem under consideration, one has quasiorthogonality of L modes and pseudohermiticity of operator $\hat{L}_\perp$, there should exist a certain operator $\hat{\mathcal{C}}$ that the action of $\hat{\mathcal{C}}$ together with the $\mathcal{PT}$ transformation will give the hermiticity condition and real-quantity energy eigenstates. A form of operator $\hat{\mathcal{C}}$ is found from an assumption that operator $\hat{\mathcal{C}}$ acts only on the boundary conditions of the L-mode spectral problem. Such a technique was used in Refs. [23,36].

Operator $\hat{\mathcal{C}}$ is a special differential operator in the form of $i\frac{\mu_a}{\Re}(\vec{\nabla}_\theta)_{r=\Re}$. Here, $(\vec{\nabla}_\theta)_{r=\Re}$ is the spinning-coordinate gradient. It means that, for a given direction of a bias field, operator $\hat{\mathcal{C}}$ acts only for a one-directional azimuth variation. The eigenfunctions of operator $\hat{\mathcal{C}}$ are double-valued border functions [23,36]. This operator allows performing the transformation from the natural boundary conditions of the L modes, expressed by Eqs. (8) and (11), to the essential boundary conditions of the so-called G modes, which take the forms, respectively [19,23,28],

$$\mu\left(\frac{\partial\tilde{\varphi}}{\partial r}\right)_{r=\Re^-} - \left(\frac{\partial\tilde{\varphi}}{\partial r}\right)_{r=\Re^+} = 0, \tag{29}$$

and

$$(-\mu)^{1/2}\left(\frac{J_\nu'}{J_\nu}\right)_{r=\Re} + \left(\frac{K_\nu'}{K_\nu}\right)_{r=\Re} = 0. \tag{30}$$

The membrane functions of the G modes are related to the orbital-coordinate system. It is evident that the quantumlike G-mode spectra cannot be shown by the HFSS numerical simulation. Using operator $\hat{\mathcal{C}}$, we construct the new inner product structure for boundary functions,

$$(\tilde{\varphi}_n|_{r=\Re},\tilde{\varphi}_m|_{r=\Re}) = \oint_{\mathcal{L}} [\hat{\mathcal{C}}\mathcal{PT}\tilde{\varphi}_m|_{r=\Re}(z)][\tilde{\varphi}_n|_{r=\Re}(z)]d\ell. \tag{31}$$

As a result, one has the energy eigenstate spectrum of MS-mode oscillations with topological phases accumulated by the double-valued border functions [23]. The topological effects

become apparent through the integral fluxes of the pseudoelectric fields. There are positive and negative fluxes corresponding to the counterclockwise and clockwise edge-function chiral rotations. For an observer in a laboratory frame, we have two oppositely directed anapole moments $\vec{a}^e$. This anapole moment is determined by the term $i\frac{\mu_a}{\Re}(\frac{\partial\bar{\varphi}}{\partial\theta})_{r=\Re^-}$ on the right-hand side of Eq. (8). For a given direction of a bias magnetic field, we have two cases $\vec{a}^e \cdot \vec{H}_0 > 0$ and $\vec{a}^e \cdot \vec{H}_0 < 0$. As supposed [23], the magnetoelectric energy splitting should be observed, which is, in fact, the splitting due to spin-orbit interaction.

The numerically observed topologically distinctive split-resonance states of the MDM-vortex-polariton structures are due to the $\mathcal{PT}$-invariance properties of operator $\hat{L}_\perp$. Such properties are evident, in particular, from a strong variation of a geometric phase against the background on a nonvarying dynamical phase. Contrary to the quasiorthogonality of the L modes, for the G modes, one has the hermiticity condition and the real-quantity energy eigenstates. Based on the above analysis, one can conclude that frequency differences for peak positions of the analytically derived L and G modes should be on the same order of magnitude as the frequency differences for the split-resonance states observed in the HFSS spectrum. Figure 17, showing spectrum peak positions for the HFSS simulation and the analytical L and G modes, gives evidence for this statement.

IV. CONCLUSION

Small ferrite-disk particles with MS oscillations are characterized by topologically distinctive long-living resonances with symmetry breakings. While for an incident electromagnetic wave, there is no difference between the left and the right, in the fields scattered by a MDM ferrite particle, one should distinguish left from right. It was shown that, due to MDM vortices in small thin-film ferrite disks, there is strong magnon-photon coupling. The coupled states of electromagnetic fields with MDM vortices are characterized by different topological properties. Numerically, we showed that scattering of electromagnetic fields from such small ferrite particles gave the topological-state splitting. For topologically distinctive structures of MDM-vortex polaritons, one has localization or cloaking of electromagnetic fields. An essential feature of the MDM-vortex polaritons is the presence of the local circular polarization of the fields together with the cyclic propagation of electromagnetic waves around a disk axis. This geometric-phase effect is intimately related to the hidden helical properties of MDMs.

A small ferrite disk with MDM spectra, placed in a standard microwave structure, represents a nonintegrable electromagnetic problem. While this problem can be well solved numerically, there is also the possibility for using an analytical approach. In this approach, a spectral problem for MDM resonances is formulated based on special macroscopic scalar wave functions—the MS-potential wave functions ψ. The study of symmetry and topological properties of MS-potential wave functions ψ in quasi-2D ferrite disks gives necessary theoretical insight into the origin of the MDM-vortex-polariton structures. This analytical study explains the numerically observed topological textures of the fields of MDM-vortex polaritons. Based on the ψ-function analysis, we demonstrated such very important spectral properties of MDMs in quasi-2D ferrite disks as helical resonances and the $\mathcal{PT}$ invariance. We showed that there exists a special differential operator, acting on the boundary conditions of the spectral problem, which allows obtaining the hermiticity condition and the real-quantity energy eigenstates for MDMs.

In recent years, we were witnesses to a resurgence of interest in spin-wave excitations motivated by their possible use as information carriers (see Ref. [39] and references therein). Technological opportunities lend further momentum to the study of the fundamental properties of spin-wave oscillations and the interaction of these oscillations with electromagnetic fields. Among different types of microwave magnetic materials, YIG is considered as one of the most attractive materials due to its uniquely low magnetic damping. This ferrimagnet has the narrowest known line of ferromagnetic resonance, which results in a magnon lifetime of a few hundred nanoseconds. The interaction of microwave fields with MDM vortices opens a perspective for creating different electromagnetic structures with special symmetry properties. The shown properties of MDMs in a quasi-2D ferrite disk offer a particularly fertile ground in which $\mathcal{PT}$-related concepts can be realized and can be investigated experimentally. The important reasons for this are as follows: (a) the formal equivalence between the quantum mechanical Schrödinger equation and the G-mode MS-wave equation [23] and (b) the possibility to manipulate the ferrite-disk geometrical and material parameters and the bias magnetic field. One of the examples of different MDM-polariton structures could be $\mathcal{PT}$ metamaterials. There is also another interesting aspect. Since MDM vortices are topologically stable objects, they can be used as long-living microwave memory elements.

[1] S. M. Bose, E-N. Foo, and M. A. Zuniga, Phys. Rev. B **12**, 3855 (1975).

[2] C. Shu and A. Caillé, Solid State Commun. **34**, 827 (1980).

[3] L. Remer, B. Lüthi, H. Sauer, R. Geick, and R. E. Camley, Phys. Rev. Lett. **56**, 2752 (1986).

[4] R. L. Stamps, B. L. Johnson, and R. E. Camley, Phys. Rev. B **43**, 3626 (1991).

[5] T. Dumelow, R. E. Camley, K. Abraha, and D. R. Tilley, Phys. Rev. B **58**, 897 (1998).

[6] S. S. Gupta and N. C. Srivastava, Phys. Rev. B **19**, 5403 (1979).

[7] A. S. Akyol and L. E. Davis, in *Proceedings of the 31st European Microwave Conference* (European Microwave Association, London, 2001), Vol. 1, pp. 229–232.

[8] P. So, S. M. Anlage, E. Ott, and R. N. Oerter, Phys. Rev. Lett. **74**, 2662 (1995).

[9] M. Vraničar, M. Barth, G. Veble, M. Robnik, and H.-J. Stöckmann, J. Phys. A: Math. Gen. **35**, 4929 (2002).

[10] H. Schanze, H.-J. Stöckmann, M. Martinez-Mares, and C. H. Lewenkopf, Phys. Rev. E **71**, 016223 (2005).

[11] A. G. Gurevich and G. A. Melkov, *Magnetic Oscillations and Waves* (CRC, New York, 1996).

[12] E. O. Kamenetskii, M. Sigalov, and R. Shavit, Phys. Rev. E **74**, 036620 (2006).
[13] M. Sigalov, E. O. Kamenetskii, and R. Shavit, Phys. Lett. A **372**, 91 (2008).
[14] M. Sigalov, E. O. Kamenetskii, and R. Shavit, J. Appl. Phys. **103**, 013904 (2008).
[15] J. F. Dillon Jr., J. Appl. Phys. **31**, 1605 (1960).
[16] T. Yukawa and K. Abe, J. Appl. Phys. **45**, 3146 (1974).
[17] E. O. Kamenetskii, M. Sigalov, and R. Shavit, Phys. Rev. A **81**, 053823 (2010).
[18] M. Sigalov, E. O. Kamenetskii, and R. Shavit, J. Phys.: Condens. Matter **21**, 016003 (2009).
[19] E. O. Kamenetskii, M. Sigalov, and R. Shavit, J. Appl. Phys. **105**, 013537 (2009).
[20] R. Y. Chiao and Y. S. Wu, Phys. Rev. Lett. **57**, 933 (1986); A. Tomita and R. Y. Chiao, *ibid.* **57**, 937 (1986); M. V. Berry, Nature (London) **326**, 277 (1987).
[21] K. Y. Bliokh and D. Y. Frolov, Opt. Commun. **250**, 321 (2005).
[22] E. O. Kamenetskii, J. Phys.: Condens. Matter **22**, 486005 (2010).
[23] E. O. Kamenetskii, J. Phys. A: Math. Theor. **40**, 6539 (2007).
[24] U. Leonhardt and P. Piwnicki, Phys. Rev. A **60**, 4301 (1999).
[25] L. Allen, M. W. Beijersbergen, R. J. C. Spreeuw, and J. P. Woerdman, Phys. Rev. A **45**, 8185 (1992).
[26] A. T. O'Neil, I. MacVicar, L. Allen, and M. J. Padgett, Phys. Rev. Lett. **88**, 053601 (2002).
[27] Y. Ohdaira, T. Inoue, H. Hori, and Kitahara, Opt. Express **16**, 2915 (2008).
[28] E. O. Kamenetskii, Phys. Rev. E **63**, 066612 (2001).
[29] E. O. Kamenetskii, M. Sigalov, and R. Shavit, J. Phys.: Condens. Matter **17**, 2211 (2005).
[30] R. A. Waldron, Q. J. Mech. Appl. Math. **11**, 438 (1958).
[31] E. O. Kamenetskii, J. Magn. Magn. Mater. **302**, 137 (2006).
[32] C. M. Bender, Rep. Prog. Phys. **70**, 947 (2007).
[33] E. J. Galvez, P. R. Crawford, H. I. Sztul, M. J. Pysher, P. J. Haglin, and R. E. Williams, Phys. Rev. Lett. **90**, 203901 (2003).
[34] S. G. Mikhlin, *Variational Methods in Mathematical Physics*, International Series of Monographs in Pure and Applied Mathematics, 50 (Oxford-London-Edinburgh-New York-Paris-Frankfurt: Pergamon Press, 1964).
[35] M. A. Naimark, *Linear Differential Operators* (Ungar, New York, 1967).
[36] E. O. Kamenetskii, Phys. Rev. E **73**, 016602 (2006).
[37] C. M. Bender, D. C. Brody, and H. F. Jones, Phys. Rev. Lett. **89**, 270401 (2002).
[38] G. S. Japaridze, J. Phys. A: Math. Gen. **35**, 1709 (2002).
[39] A. A. Serga, A. V. Chumak, and B. Hillebrands, J. Phys. D: Appl. Phys. **43**, 264002 (2010).